Response of Articular Human Adult Chondrocytes to a Non-fouling RGD-peptide Modified Surface –

A Comparative Study *vs.* Tissue Culture Treated Polystyrene

Master Thesis in Nanosciences

Daniel Vonwil

University of Basel
2006

Research Mentors**:** Prof. Dr. Ueli Aebi (Biozentrum, University of Basel, MIH)

Dr. Andrea Barbero (Universitiy Hospital Basel, ICFS)

TABLE OF CONTENTS

1 ABBREVIATIONS

AHACs	Adult human articular chondrocytes
AFM	Atomic force microscopy
CLSM	Confocal laser scanning microscopy
CM	Culture Medium
DMEM	Dulbecco's modified Eagle's medium
ECM	Extracellular matrix
FBS	Fetal bovine serum
FGF-2	Fibroblast growth factor 2
GAG	Glycosaminoglycanes
HEPES	N-(2-Hydroxyethyl)piperazine-N′-(2-ethanesulfonic acid)
ITS	Insulin/Transferrin/Selenium
PBS	Phosphate-buffered saline
PEG	PLL-*g*-PEG; poly (ethylene glycol) grafted on PLL
PLL	Poly-(L)-lysine
PDGF-BB	Platelet derived growth factor type BB
RGD	PLL-*g*-PEG/PEG-RGD, (RGD; cell adhesion ligand)
S	Stiffness
TCPS	Tissue culture treated polystyrene
TFP	Growth factor mix TGF- ß1, FGF-2 and PDGF-BB
TGF-ß1	Transforming growth factor 1
ϕ	Shape factor (Phi)
ϕ_A	Average shape factor

2 ABSTRACT

Adult human articular chondrocytes (AHACs) were analyzed for their response to a non-fouling RGD-peptide modified surface (RGD) in a comparative study *vs*. tissue culture treated polystyrene (TCPS). Beyond attachment and proliferation, AHACs were characterized for their morphology, motility, elasticity and expression of chondrogenic genes during expansion. Moreover, the ability to form cartilaginous matrix after expansion on the modified surface was determined in an *in vitro* chondrogenic assay (pellet culture).

In comparison to TCPS, AHACs during expansion on the RGD-modified surface, showed a higher expression of the chondrogenic marker collagen II mRNA. Furthermore on RGD, AHACs formed more filopodia but tended to be slightly less motile than on TCPS. In the subsequent *in vitro* chondrogenic assay, however the found differences for collagen II mRNA were not reflected. Furthermore, the formed, cartilaginous matrix of the pellets generated from AHACs expanded on RGD did not differ from that of pellets obtained from AHACs expanded on TCPS.

The surface-cell interaction of AHACs, as it appears to be specifically mediated by the dodecapeptide of the RGD-functionalized PLL-*g*-PEG, is the prerequisite for cell attachment and subsequent proliferation. Moreover it also seems, that the interaction of the integrins with the RGD-functionalized surface supports the chondrogenic phenotype during expansion of AHACs in a 2D layer. However, this effect does not seem to be sustained in the absence of the RGD-modified surface in the subsequent pellet culture. Thus, ongoing work should include RGD-modified surfaces in a 3D *in vitro* chondrogenic assay.

INTRODUCTION

Numerous synthetic polymers have been designed for tailored surface modifications in medical application and the effect of these polymer surfaces has been investigated in many *in vitro studies*. Yet, the cells used for testing are mostly from animal sources and the performed analysis largely focuses on attachment and proliferation (Hersel et al., 2006). Furthermore, only few results are published, which describe the effect of tailored synthetic polymers on chondrocytes (Grimmer et al., 2004; Hersel et al., 2006; Hsu et al., 2004; Ji et al., 2004; Kim et al., 2002).

Chondrocyte differentiation is strongly dependent on the extracellular matrix (ECM). In particular, the maintenance of normal cartilage structure has been shown to require the interaction of the cell-adhesion receptor α5β1 integrin, with ECM-ligands through an arginine-glycine-aspartic acid (RGD) sequence. Blocking of α5β1 integrin by specific antibodies or soluble RGD peptide induces inhibition of prehypertrophic chondrocyte differentiation and partially leads to apoptosis (Garciadiego-Cázares et al., 2004).

The integrins consist of two non-covalently associated transmembrane subunits, termed α and β. So far, 18 α and 8 β subunits have been found which form 24 different heterodimers. Through the combination of a particular α and β subunit the integrins determine their ligand specifity (van der Flier and Sonnenberg, 2001).
The process of integrin-mediated cell adhesion comprises a cascade of four different, partly overlapping events. Firstly, in the initial attachment step the cell

contacts the surface and some ligand binding occurs that allows the cell to withstand gentle shear forces. Secondly, the cell body begins to flatten and its plasma membrane spreads over the substrate. Thirdly, this leads to actin organization into microfilament bundles referred to as stress fibres. In the fourth step, the formation of focal adhesions occurs, which link the ECM to molecules of the cytoskeleton (Lebaron and Athanasiou, 2000).
The cytoskeleton consists of a force bearing, filamentous protein network which largely determines the cell' s mechanical properties. The three major components are actin microfilaments, microtubules and intermediate filaments. During spreading after integrin-mediated cell adhesion, cell shape changes occur. This process involves the transfer of mechanical forces between the cytoskeleton and the ECM as well as changes in viscoelasticity (Stamenovic´ and Wang, 2000).

The viscoelasticity of single cells can be determined through indentation-type atomic force microscopy. This technique has been used to determine rheology of several cell lines, including human lung epithelial cells and rat liver macrophages (Rotsch et al., 1997;Zhu et al., 2000). Cells exhibit both solid and liquid like features, i.e., they are visoelastic. As such, cells store and dissipate mechanical energy and their response to mechanical stimuli depends on the rate at which the stimulus is applied (Zhu et al., 2000). There are two mechanisms responsible for this behaviour; a flow-independent mechanism, intermolecular friction, exhibited in all polymeric materials (e.g. cytoskeleton: made of biopolymers) and a flow-dependent mechanism that is present if loading conditions allow water to move through the probed structure (Stolz et al., 2004).

Twenty years ago, Pierschbacher and Ruoslahti identified the RGD tripeptide motif in their attempt to reduce the known macromolecular cell adhesion ligand, fibronectin, to a small recognition sequence (Pierschbacher and Ruoslahti, 1984).

This breakthrough has opened the door for the creation of new biomaterials by presenting cell recognition motifs as small immobilized peptides (Hersel et al., 2003). Despite the inherent biological properties of natural ECM proteins, issues including complexities associated with purification, immunogenicity and pathogen transmission have spurred the development of synthetic biomaterials (Lutolf and Hubbell, 2005). Today, the RGD sequence is by far the most effective and most often employed peptide sequence for stimulated cell adhesion on synthetic surfaces (Hersel et al., 2003).

Many different polymer systems have been developed to immobilize peptide sequences onto biomaterial surfaces (Hersel et al., 2003). However, most of them lack the ability of being protein-resistant (Morra, 2000). As a consequence, proteins present in the media or blood serum adsorb to the surface and can interfere with the study of peptide-integrin interaction. One way to avoid this problem is the use of the poly(L-lysine)-graft-poly(ethylene glycol) (PLL-*g*-PEG) molecular assembly system (Huang et al., 2000;Kenausis et al., 2000;Tossati et al., 2003). In detail, the poly-L-lysine backbone, which at pH 7.4 is positively charged, can bind electrostatically to a negatively charged surface i.e. tissue culture treated polystyrene. The poly(ethylene glycol) (PEG) spacer blocks adsorption of serum proteins and can be functionalized with bioligands, i.e. RGD (VandeVondele, 2003). The binding of integrins to this recognition sequence is not only responsible for cell adhesion but also plays an important role in cell differentiation (Ruoslahti and Pierschbacher, 1997).

In recent years, chondrocytes have received great attention in context with cell-based repair of cartilage which has a limited capacity for self-healing (Sittinger et al., 1999). Garciadiego-Cázares (2004) reported that the maintainance of chondrocytes' phenotype strongly depends on their interaction with RGD in the

ECM. Based on this finding, the objective of this study was to investigate the response of adult human articular chondrocytes (AHACs) to a non-fouling RGD-peptide modified surface. To allow for specific interaction with the chondrocytes' integrins, an RGD-functionalized PLL-*g*-PEG copolymer was chosen. It was hypothesized, that by presenting this tailored RGD-modified surface to the AHACs, their ability to from cartilaginous tissue would be enhanced. Thus, in this study the response of AHACs to a non-fouling RGD-peptide modified surface was investigated beyond attachment and proliferation. AHACs were also characterized for their morphology, motility, elasticity and expression of chondrogenic genes during expansion. Moreover, the ability to form cartilaginous matrix after expansion on the RGD-modified surface was determined in an *in vitro* chondrogenic assay (pellet culture).

4 ORGANIZATION OF THE THESIS

The idea for this thesis arose during a written assignment for a lecture on extracellular matrix. In this context, a project proposal has been written, together with PhD student S. Ströbel (ICFS, University Hospital Basel), that lead to the present master thesis. Following, a brief overview of the experimental design and the collaborations is given.

4.1 EXPERIMENTAL DESIGN

Articular human chondrocytes (AHACs) were isolated from articular cartilage biopsies. The isolated chondrocytes were frozen after 4h of adhesion on tissue culture treated dishes (TCPS). Expansion occurred on conventional TCPS and TCPS modified with either RGD-functionalized PLL-*g*-PEG (RGD) or PLL-*g*-PEG (PEG) only. Where TCPS was chosen as standard condition, PEG served as a negative control of RGD. The expansion occurred in two steps to allow for a sufficient number of AHACs needed for subsequent analysis.

During expansion, the attachment, proliferation and mRNA (Coll I, II & X) expression profile of AHACs was analyzed. A fraction of the expanded AHACs was pelleted and cultured in chondrogenic medium for two weeks. To assess the AHACs' *post* expansion chondrogenic capacity, the obtained pellets were analyzed for mRNA expression levels, GAG/DNA and histology (GAG and Coll II). The remaining fraction of the expanded AHACs was stored in liquid nitrogen. From this stock, cells were reseeded correspondingly onto either TCPS or RGD. Under these expansion conditions, AHACs were analyzed for their morphology (CLSM and AFM), rheology (AFM) and motility (time lapse microscopy).

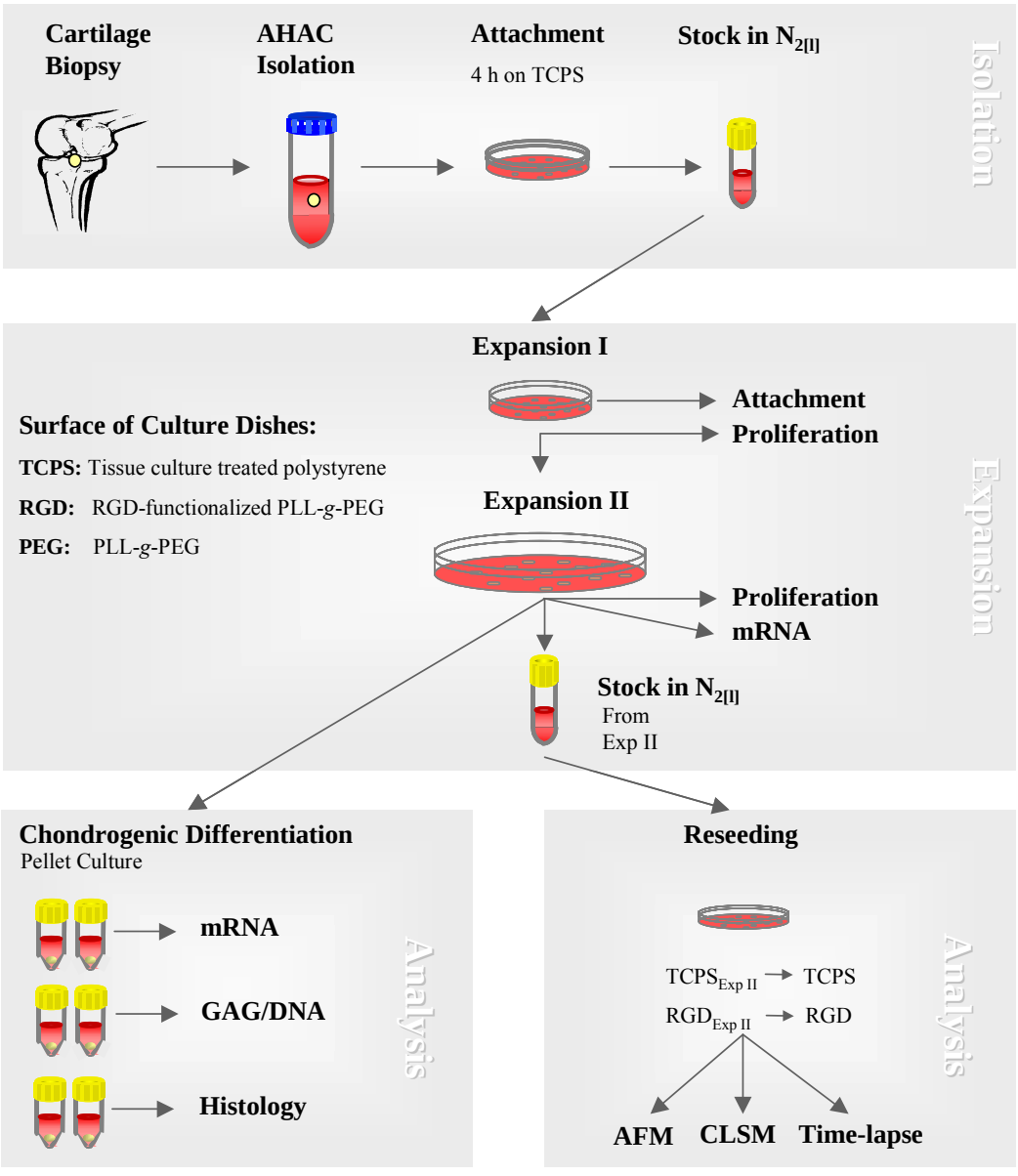

FIGURE 4.1 Schematic view of the experimental design used in this study.

4.2 COLLABORATIONS

Three different groups have contributed to the work presented in this thesis. At the beginning of the thesis, the polymers required for the surface modifications RGD and PEG could be obtained in collaboration with the Material Sciences group of Prof. Dr. M. Textor (ETHZ). From this group, PhD student M. Schuler has synthesized and characterized the polymer used in this thesis. Furthermore, he provided me with the protocols for the application of the polymers. Next, cell culture on the modified surfaces and subsequent analysis was done in the Tissue Engineering laboratory of PD Dr. I. Martin (ICFS, University Hospital Basel). There, Dr. A. Barbero was supporting me in most aspects of this thesis. In a final step of the thesis, the effect of the modified surfaces was investigated by atomic force (AFM) microscopy and confocal laser scanning microscopy (CLSM). This complementary analysis was performed in the group of Prof. Dr. U. Aebi at the M. E. Muller Institute (University of Basel).

5 MATERIALS & METHODS

5.1 SURFACE PREPARATION

In this thesis, AHACs were cultured and characterized on three different surfaces; **i)** tissue culture treated polystyrene (TCPS), **ii)** a protein repelling, cell adhesion mediating surface (RGD) and **iii)** the same protein repelling surface but without the integrin-specific bio ligand RGD (PEG). For simplicity the three different surface conditions are referred to by their abbreviation; TCPS, RGD and PEG.

5.1.1 Description of the different surfaces

TCPS was used as a substrate and **i)** for the standard condition left untreated as it is currently applied for *in vitro* expansion of AHACs. TCPS dishes and flasks were bought from TPP (Tarasdingen, Switzerland) where they are manufactured by exposing the polystyrene surface to an atmospheric plasma that renders the surface hydrophilic (according to technical support from TPP). Onto this surface, cell adhesion mediating proteins (e.g. fibronectin) from the FBS containing culture medium can adsorb.

At a pH of 7.4, TCPS exhibits negative charges onto which poly-(L)- lysine (PLL) grafted copolymers in buffer solution can be adsorbed electrostatically. **ii)** To investigate the influence of the integrin-specific cell adhesion sequence RGD on the characteristics of AHACs, TCPS was coated with RGD-modified PLL-*g*-PEG (see table. 5.1, synthesized and characterized by Martin Schuler, material sciences ETH Zürich). This graftcopolymer consists of two different PEG chains (2 kDa, 3.4 kDa) grafted onto a PLL backbone. The grafting ratio *g* was one PEG chain per seven lysine units. The PEG chains were either short (2 kDa) and non-

functionalized, or long (3.4 kDa) and terminated with an RGD-containing dodecapetide (N-Acetyl-GCGRGYG**RGD**SPG-amide). The percentage of functionalized PEG chains relative to the total amount of PEG chains was 1 %. **iii)** As a negative control, PLL-*g*-PEG with PEG chains of 2 kDa (47 ethylene glycol monomers) was used (Tosatti, 2005;Vande Vondele et al., 2003).

TABLE 5.1 Overview of different surface conditions, with the codes used in this thesis. Where *g* indicates the PEG grafting per PLL, x expresses the fraction of RGD-functionalised PEG chains

Code	Full name	Short name	PLL-*g*-PEG/PEG-RGD-*x*%	RGD/cm^2	Serum adsorption to surface
TCPS	Tissue culture treated polystyrene	TCPS	-	?	?
RGD	RGD functionalized - Poly-(L-lysine)-*g*-poly(ethylene glycol)	PLL-*g*-PEG/PEG-RGD	*g* = 7.0 *x* = 1%	2.04 pmol	< 5ng/cm^2
PEG	Poly-(L-lysine)-*g*-poly(ethylene glycol)	PLL-*g*-PEG	*g*= 3.3	-	< 5ng/cm^2

5.1.2 Preparation & characteristics of the RGD and PEG of the surface

The polymers were dissolved in 10 mM HEPES, 150 mM NaCL buffer (pH 7.4) at a concentration of 0.5 mg/ml and sterile filtered through a 0.22 μm filter. To avoid repetitive freezing (leading to hydrolysis) and thawing, the polymer solutions were divided into the calculated aliquots and stored at –20°C until use. The chosen concentration is 5000 times higher than that needed for the formation of a monomolecular adlayer. Based on quantitative NMR data of the polymer

(grafting ratio g and fraction of RGD-functionalized PEG chains) and the average optical waveguide lightmode spectroscopy (OWLS; adsorbed polymer mass), the RGD concentration on TCPS was calculated to be 2.04 pmol/cm^2 (Schuler et al., 2006). The non-specific serum protein adsorption onto both, the PEG and the RGD grafted polymer surface was measured to be below 5 ng/cm^2 as typically found for PLL-g-PEG polymers (Tosatti, 2005).

The copolymer solutions described above were thawed and filled into TCPS flasks at a ratio of 100 µl/cm^2. The flasks were stirred on an orbital shaker at room temperature for 45 min. The supernatant polymer solution was aspirated and the coated, as well as the non-coated surfaces, were washed twice with HEPES buffer for 5 min with a ratio of 200 µl/cm^2. All open liquid handling was performed in a laminar flow box.

5.2 CELL CULTURE

5.2.1 Isolation of AHACs

Full thickness human articular cartilage samples were collected within 24 hours *post mortem* from the femoral lateral condyle of three different donors (age in years; A:53, B:62, C:66), with no history of joint disease, after obtained informed consent and in accordance with the local ethical commissions.

AHACs were isolated by digestion the biopsies with 0.15% type II collagenase for 22 hours. The digested cartilage was strained through a 200 µm filter, centrifuged and resuspended with Dulbecco's modified Eagle's medium

(DMEM) containing 4.5 mg/ml D-glucose, 0.1 mM nonessential amino acids, 1 mM sodium pyruvate, 100 mM HEPES buffer, 100 U/ml penicillin, 100 µg/ml streptomycin, and 0.29 mg/ml L-glutamine, supplemented with 10% FBS (culture medium, CM) at the density of 10 000 cells/cm^2. This cell suspension was plated in a TCPS dish for 5 hours at 37°C to allow for primary attachment. Following, the cells were detached with 0.05% trypsin/0.52 mM EDTA and frozen as described below.

5.2.2 Freezing of AHACs

The AHACs harvested from the primary attachment were centrifuged and the CM supplemented with TFP replaced by 0°C freezing medium I (FM I) to give a cell density of $2x10^6$ cells/ml. The FM I contained Dulbecco's modified Eagle's medium containing 4.5 mg/ml D-glucose, 0.1 mM nonessential amino acids, 1 mM sodium pyruvate, 100 mM HEPES buffer, 100 units/ml, 100 µg/ml streptomycin, and 0.29 mg/ml L-glutamine, supplemented with 20 vol-% FBS. To this cell suspension an equivalent volume of freezing medium II (FM II) was added at 0°C very slowly. FM II is of the same composition as FM I but additionally contains 20 vol-% DMSO.

Aliquots of $5x10^5$ cells/vial were prepared, placed in cryo freezing container filled with 0°C Isopropanol and stored in the –70°C freezer for 24 hours. Subsequently, the AHACs were transferred to the liquid nitrogen storage

5.2.3 Thawing of AHACs

AHACs removed from the liquid nitrogen storage, were thawed in a 37°C water bath, immediately diluted 35 fold in CM of 37°C and allowed to stand at this temperature for 10 min. Following, this suspension was centrifuged, and the supernatant replaced by CM supplemented with TFP.

5.2.4 Expansion of AHACs

Primary adult human articular chondrocytes (AHACs) were taken from the liquid nitrogen stock and expanded on TCPS, RGD and PEG (polymer coating of the substrate as described above) in two subsequent steps.

For the first expansion phase, AHACs of each donor were inoculated onto either TCPS, RGD or PEG surface presenting dishes at 10^4 cells/cm^2. The AHACs were cultured in CM supplemented with 1 ng/ml TGF-ß1, 5 ng/ml FGF-2, 10 ng/ml PDGF-BB (TFP) in a humified 37°C/5% CO_2 incubator. The growth factor combination TFP was selected based on the reported ability to increase AHAC proliferation and redifferentiation capacity (Barbero et al., 2004).

When the AHACs reached the first confluency (first expansion step) they were detached by treatment with 0.3% type II collagenase, followed by 0.05% trypsin/0.52 mM EDTA, counted in a Neubauer chamber (staining of dead cells with Trypan blue) and re-plated for the second expansion step. Therein, AHACs were seeded into a correspondingly coated dish at 5 x10^3 cells/cm^2 and cultured in CM and growth factor medium TFP in a humified 37°C/5% CO_2 incubator.
Confluently grown AHACs from expansion step II were detached and frozen (described above) for latter analysis (CLSM, AFM, time lapse). A fraction of the detached cells was immediately pelleted and cultured in chondrogenic medium (see chondrogenic differentiation).

5.3 ANALYSIS OF THE SURFACE EFFECT ON AHACs

5.3.1 Determination of cell attachment & proliferation-rate

To determine the cell attachment, 24 hours after inoculation (expansion step I), the supernatants containing the non-adherent cells were collected, concentrated and counted.
The cell proliferation-rate was determined at the end of each expansion step

The supernatant from each well/flask was collected and the empty wells rinsed three times with PBS. The PBS was united with the corresponding supernatants and the empty wells immediately refilled with TFP medium.
The collected volumes were centrifuged at 1400 rpm for 3 min. Aliquots of the concentrates were used to count the cells in a Neumann chamber and the cell mortality was checked by using Trypan blue. The non-adherent AHACs from TCPS and RGD were discarded whereas for the PEG, the cells were returned to the well/flask where they were diluted with TFP to restore the previous cell density. The percentage of floating cells (dead and alive) was calculated relative to the number of initially inoculated cells and subtracted from 100% to give the percentage of attached cells. The results are presented with a standard deviation to indicate the interdonor variability.
The cell proliferation-rate was determined at the end of each expansion step and reported as total proliferation index. This index can be calculated from the sum of doublings during both expansion steps, divided by the number of days in expansion. The doubling is the $\log_2$ of the ratio between the number of cells after expansion and the number of inoculated cells.

5.3.2 Analysis of AHAC morphology by confocal microscopy

AHACs, frozen after expansion step II, were thawed and seeded onto TCPS and RGD. The adherently grown AHACs, were fixed, permeabilized and labelled for actin and the nucleus prior to image acquisition with the confocal laser scanning microscope (CLSM).

5.3.2.1 Fixation & permeabilization of AHACs

AHACs were adherently grown on TCPS or RGD using 13 mm diameter Thermanox® lamellae (Nunc, USA) as a substrate. The Thermanox® were activated prior to their use by placing them in a UVO-Cleaner (Model 42-220, Jetlight Company, USA) for 30 min. The activated Thermanox® surfaces were coated as described above.
Frozen AHACs from expansion step II, on either TCPS or RGD, were thawed, seeded onto a correspondingly coated lamellae at 5 $x10^3$ cells/cm^2 and cultured in TFP medium in a humified 37°C/5% CO_2 incubator.

After three days of culture, the lamellae were transferred to a clean 12-well plate where they were rinsed with 37°C cell buffer (CB) containing 137 mM NaCl, 5mM KCl, 1.1 mM $Na_2HPO_4x12\ H_2O$, 0.4 mM KH_2PO_4, 5.5 mM glucose, 4 mM $NaHCO_3$, 2 mM $MgCl_2$, 2 mM EGTA, 5 mM MES. Then, the AHACs were fixed with 1 % glutaraldehyde in CB for 30 min. at room temperature. The lamellae were rinsed with room temperature CB before permeabilizing and further fixing the AHACs with 2 % Octyl-polyethylene (Octyl-POE) and 0.125 % glutaraldehyde for 5 min. After rinsing with CB, the remaining surplus

glutaraldehyde was reduced with a solution of 0.5 g/ml $NaBH_4$ in CB at 0°C for 20 min. In a final step, the lamellae were washed with CB at RT. Great attention was paid to never let the lamellae dry and to avoid fluid flow directly onto the lamellae.

5.3.2.2 Labelling of AHACs

The permeabilized and fixed cells were incubated for 30 min in cell buffer containing a combination of TRITC-phalloidin 1:900 (λ_{Ex} 488 nm, Sigma) against actin filaments and DRAQ5 1:200 (λ_{Ex} 647 nm, Alexis Biochemicals) to label DNA in the nuclei.

5.3.2.3 Embedding of AHACs for confocal microscopy

On a glass carrier slide, each lamella (with the labelled cells on top) was mounted onto a drop of mowiol-1188 (Hoechst, Frankfurt, Germany) containing 0.75 % of the anti-fading agent N-propyl-gallate. Without letting the surface dry out, the lamellae was covered with another drop of mowiol before sealing it with a cover glass (0.17 mm thickness). The samples were allowed to dry over night at 4 °C in the dark and stored under these conditions up to their analysis by CLSM.

FIGURE 5.1 Schematic view of sample embedding for CLSM

5.3.2.4 CLSM image acquisition

AHACs, labelled for actin filaments and the nuclei were visualized with a Leica TCS SP CLSM.

The 63x HC PL APO immersion objective was chosen for studying morphological features and to acquire images for the shape factor determination of AHACs. The number of stacks was fixed to 20 while each stack (1024x1024 pixels) was scanned at medium speed and averaged four times.

5.3.2.5 Shape factor & image analysis

To describe the AHAC's morphology and the degree of spreading, a cell shape factor ϕ (Phi) was used, this is defined as:

$$\phi = \frac{4 \cdot \pi \cdot A}{p^2} \qquad \textbf{Equation 5.1}$$

where A is the cell footprint area and p is the perimeter of the cell. The shape factor for a round cell can assume values near to one. Circles have the greatest area-to perimeter ratio and their shape factor ϕ is 1, whereas a thin, thread-like object would have a shape factor ϕ near 0 (Schuler et al., 2006).

The area and the perimeter of AHACs were determined from the CLSM images in Image J. The shape factor ϕ is reported as the average value ϕ_A from 30 measured AHACs for each condition.

5.3.3 Time lapse microscopy of AHACs

The motility of AHACs on the two different surfaces, TCPS and RGD was analysed by time lapse microscopy in phase contrast over a time span of 7 hours.

AHACs, frozen after expansion step II, were thawed and inoculated into a twelve well plate with two wells presenting TCPS and another two wells presenting RGD at their surface. The AHACs were seeded at an initial density of 7500 cells/cm^2 and cultured in TFP medium. The twelve well plate was kept in a box enclosing the microscope. In this box, a humidified atmosphere with 37°C/5% CO_2 was maintained.
Twenty four hours *post* inoculation, the acquisition of 144 images with a time interval of 5 min. was started. During each interval, the twelve well plate was sequentially moved from well to well by a motorized high precision stage.

The time lapse experiments were performed on an Olympus IX81 motorized, inverted microscope, using a UplanApo 4x objective in the phase contrast mode. Additionally, the microscope was equipped with a high resolution position controller to drive the motorized stage. Images were recorded with a CCD camera. From each condition, the motility of < 100 cells was analysed throughout 80 images using the manual tracking tool of ImagePro. The average velocity is reported in nm/s.

5.3.4 Imaging and Elasticity measurements of AHACs by AFM

5.3.4.1 General AFM settings

The experiments were performed with a Nanoscope III equipped with a 120 µm scanner, a standard fluid cell, and a stereo microscope (Leica MZ16) in combination with a custom built phase contrast set up.
For imaging V-shaped 200 µm long silicon nitride cantilevers with a nominal spring constant of ~0.01 N/m (Park Scientific Instruments, Sunnyvale, CA, USA) were employed. Cell images were acquired at a scanning speed of maximally 40 µm/s in contact mode with the gains set to an instrument specific value of approximately four for both, the integral and proportional the gain. For force volume measurements, V-shaped, silicon nitride cantilevers with a nominal spring constant of ~0.03 N/m were used.
During AFM measurement, the AHACs were kept at 27°C and the TFP medium replaced every 40 min.

AFM stiffness measurements based on recording the elastic response of the chondrocytes by using the AFM tip as a nanoindenter (Stolz et al., 2004). Cyclic load-displacement curves were recorded within lamellar region (> 200 nm) of the AHACs in the force-volume mode at a vertical displacement frequency of 1 Hz. To achieve constant and well-defined maximum applied load, the maximum deflection value was set to 20 nm. This so called trigger value indicates the desired increase in photodiode voltage beyond that for the undeflected cantilever probe.

5.3.4.2 Preparation of AHACs for AFM

Two days prior to AFM analysis, AHACs from expansion step II were thawed and reseeded on TCPS and RGD lamellae at a density of 7500 cells/cm^2. The lamellae were prepared by punching out 9 mm diameter discs from Thermanox®(diamenter: 13 mm, Nunc, USA). To obtain a substrate rigidity suitable to drive high gains (integral and proportional gain of approximately 4) these lamella of 0.17 mm thickness were glued on top of 0.3 mm glass lamellae (diameter: 9 mm) with epoxy glue (Devcon, USA, two component 30 min. hardening). The compound lamllae were allowed to dry > 4 hours before placing them in a UVO-Cleaner (Model 42-220, Jetlight Company, USA) for 30 min. The activated Thermanox® surfaces were coated as described above.

5.3.4.3 AFM Data Acquisition and Processing

Each individual data set consists of 256 load-displacement curves on 25 μm^2 of an AHACs lamellar portion, whereas each curve contains 256 data points. To exclude any possible contribution from the substrate, only data from the unloading should be employed. However, due to adhesive tip-cell interaction, the shape of the unloading curve frequently showed great distortion. Thus the data for calculating the E modulus was taken from the loading curve. By use of a software programed Roberto Raiteri, an average curve was calculated from the 256 load-displacement curves.

5.3.4.4 Determination of Chondrocyte Stiffness

The elastic modulus E was approximated from the average slope (read out from a the averaged load-displacement curves) according to the modelling method developed by Oliver and Pharr (1992).

5.3.4.5 Chondrogenic Differentiation

The condrogenic capacity of AHACs expanded on either TCPS, RGD or PEG was investigated in pellet culture using a chemically defined, serum-free medium (SFM) which consists of DMEM supplemented with ITS^{+1} (Sigma Chemical, St. Louis, MO; i.e., 10 µg/ml insulin, 5.5 mg/ml transferrin, 5 ng/ml selenium, 0.5 mg/ml bovine serum albumin, 4.7 mg/ml linoleic acid), 0.1 mM ascorbic acid 2-phosphate, and 1.25 mg/ml human serum albumin 10^{-7} M dexamethasone and 10 ng/ml TGF-β1 (Barbero et al., 2003;Jakob et al., 2001).

Aliquots of $5x10^5$ cells/0.5ml were centrifuged at 250xg for 5 min. in 1.5 ml polypropylene conical tubes (Saarstedt, Nümbrecht, Germany) to form spherical pellets, which were placed onto a 3D orbital shaker (Bioblock Scientific, Frenkenkdorf, Switzerland) at 30 rpm. The pellets were cultured for 2 weeks at 37°C / 5% CO_2, with medium changes twice per week, and subsequently processed for histological and immuno-histochemical, biochemical and mRNA analysis.

5.3.5 Real-time quantitative RT-PCR assay

5.3.5.1 Total RNA extraction and complementary DNA synthesis

AHACs after expansion or pellet culture were analyzed for their expression of the chondrogenic markers collagen I, II and X as described by (Martin and Frank, 2003)

The culture medium was aspirated and the sample rinsed with PBS prior to the addition of 250 µl Trizol, which was added to inhibit RNAse activity. After that,

the samples were stored at –20°C in RNAse free tubes until the collection of samples from all conditions was complete.

The thawed samples were sonicated, vortexed with 50 µl chloroform and incubated on ice for 10 min., before they were centrifuged at 11 000 rpm/4°C for 15 minutes. The upper phase was transferred to another RNAse free tube and vortexed with 2 µl of Glycogen (20 µg/µl). From this solution, the RNA was precipitated by incubation with 125 µl isopropanol for 10 min. on ice. The samples were centrifuged at 11 000 rpm/4°C for 10 min. before the isopropanol was removed and the precipitate rinsed with 250 µl ethanol-75%. The samples were centrifuged at 11 000 rpm/4°C for 5 min. again, the ethanol removed and this washing step repeated two more times. The purified pellet was dissolved in 35 µl MilliQ, RNAse free water.

5.3.5.2 Synthesis of cDNA

The extracted RNA was treated with DNAse following the instructions of the Rneasy Kit (Ambion, Austin TX)
To estimate the purity of the extracted RNA, the absorbance of a diluted aliquot from the aqueous extract was measured with a spectrophotometer at 260 nm and 280 nm. An absorbance of 1 unit at 260 nm corresponds to 40 µg of RNA per ml. The ratio between the absorbance values at 260 and 280 nm gives an estimate of RNA purity and was accepted if higher than 1.5.

The cDNA was synthesized by starting from 5 µg of RNA, following the instructions of the Stratascript kit and using random hexamers as primers. The obtained cDNA was diluted with MilliQ water to give a final volume of 250 µl.

Primers and probes were used as described by (Barbero et al., 2003). The genes of interest were, collagen I, collagen II, collagen X, and the housekeeping gene 18-S rRNA.

5.3.5.3 Real-time RT-PCR

The reaction mix was prepared by adding into each reaction well 12.5 µl of 2x Master Mix, the required amount of primers and probe, 5 µl of cDNA and completed with water to give a total reaction volume of 20 µl. After closing the wells with the cap strips, the plate was centrifuged at 1500 rpm for 1 min.
The PCR was run with cycle temperatures and times as described by (Martin et al., 2001).
The Ct value of a real-time PCR reaction corresponds to the cycle number at which the fluorescence intensity reaches a threshold (usually, in the range 0.03-0.06). The threshold level for each set of primers and probe was selected such, that at that level all amplification curves were in their exponential phase.

5.3.5.4 Real–time RT-PCR data analysis

For each cDNA sample, the Ct value of the target gene was subtracted from the Ct value of the housekeeping gene 18-S, to derive ΔCt. This step was repeated using the cDNA from the corresponding TCPS condition as a reference, to derive Δ'Ct. After determining ΔΔCt = ΔCt - Δ'Ct, the expression level of the target gene was reported as $2^{\Delta\Delta Ct}$ (fold difference relative to the corresponding TCPS condition).

5.3.6 GAG/DNA

AHAC pellets cultured in chondrogenic medium for two weeks were digested with protease K (0.5 ml of 1 mg/ml protease K in 50 mM Tris with 1 mM EDTA, 1 mM iodoacetamide, and 10 μg/ml pepstatin-A) for 15 hours at 56°C (Hollander et al., 1994). The GAG content was measured spectrophotometrically using dimethylmethylene (Farndale R.W. et al., 1986), with chondroitin sulfate as a standard, and normalized to the DNA amount, measured spectrofluorometrically using the CyQUANT Kit (Molecular Probes, Eugene, OR), with calf thymus DNA as a standard. GAG contents are reported as μg GAG / μg DNA.

5.3.7 Histologic and Histochemical Analysis of Cell Pellets

Cell pellets cultured in chondrogenic medium were fixed in 4% formalin, embedded in paraffin, cross sectioned (5 μm thick), and stained with Safranin O for sulphated glycosaminoglycans (GAGs) (Barbero et al., 2003). The sections were also processed for immunohistochemistry to visualize collagen type II (II-II6B3, Hybrioma Bank, University of Iowa, USA) (Grogan S.P. et al., 2003).

5.4 Statistical Analysis

Statistical evaluation was performed using SPSS software (SPSS, Sigma, Stat). Values are presented as either mean±standard deviation or mean±95 %-confidence interval. Differences between the surface conditions TCPS, RGD and PEG were assessed by two-tailed Student's *t*-test for the shape factor and the motility analysis data set. The data from attachment, mortality, proliferation, mRNA expression and biochemistry experiments was analysed using the paired Mann-Whitney test.

6 RESULTS

6.1 ON RGD THE SURFACE IS MORE UNIFORM THAN ON TCPS

The surfaces TCPS, RGD and PEG were prepared for subsequent expansion of AHACs thereon. Out of these three conditions, the surface modification induced by the exposure of Thermanox® lamellae to either culture medium (TCPS condition) or a solution of the RGD-functionalized triblockcopolymer (RGD condition) was imaged by AFM. The roughness and the grain height are reported as average values over a scan area of 25 μm^2.

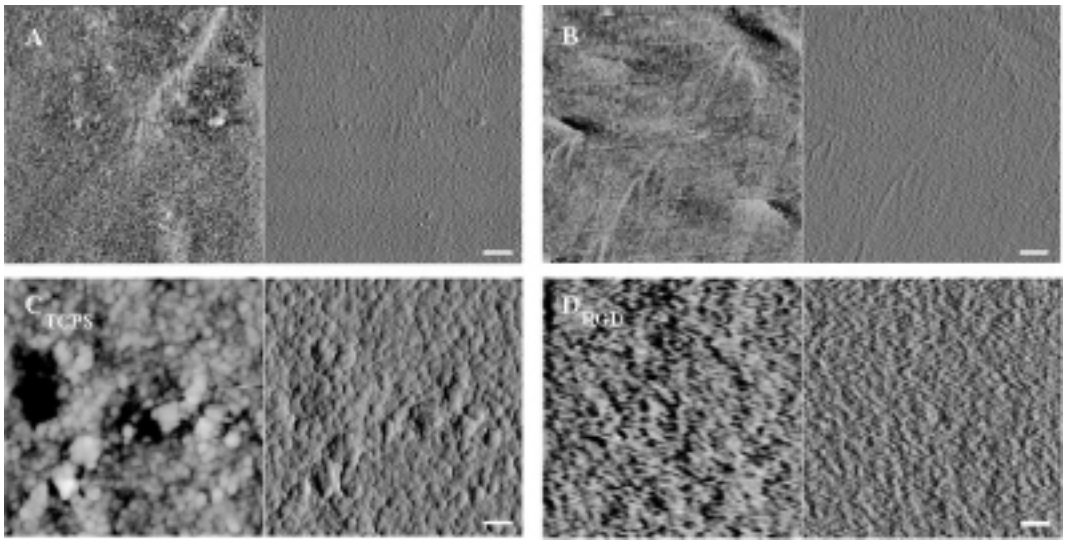

FIGURE 6.1 AFM height (left) and deflection (right) images from scans on Thermanox®, TCPS and RGD. **A** & **B** show the tissue culture treated (with atmospheric gas plasma) polystyrene surface of Thermanox® lamellae. The Thermanox® lamellae were UV cleaned prior to scanning in HEPES buffer. **C** Thermanox® lamella seen in image A after 4 hours in 10 % FBS containing culture medium (CM). This surface was scanned in CM and is referred to as TCPS condition. **D** Thermanox® lamella shown in image B after 45 min. coating with the RGD-functionalized PLL-*g*-PEG copolymer. This surface was scanned in HEPES and is referred to as RGD condition. Scale bars are 250 nm.

The surface of two individual Thermanox® lamellae as shown in image A & B of Fig. 6.1 exhibit a uniform grainy pattern with an average grain height of 10 nm and an average roughness of 1.5 nm (average values over the entire scan area). After exposing Thermanox® to culture medium, supplemented with 10% FBS, the surface assumed a cobblestone-like morphology with five-fold increased average grain height, while the average roughness was increased by a factor of four.
After adsorption of PLL-*g*-PEG/PEG-RGD from HEPES onto Thermanox®, the average grain height (12.7 nm) as well an average roughness (2.487 nm) was found nearly unaltered, while the topology showed obvious changes. The height image was dominated by a pattern of interconnected grains with blurry.

Detectable changes of surface occured by exposing Thermanox to either serum containing culture medium or a solution of RGD-functionalized PLL-*g*-PEG copolymer. Furthermore, the surface image of RGD appeared more uniform than that of TCPS.

6.2 EFFECT OF RGD-MODIFIED SURFACE ON AHACs

6.2.1 AHACs attach comparably to TCPS & RGD

Adult human articular chondrocytes (AHACs), from three different donors, were seeded onto three different surfaces; TCPS, RGD and PEG. 24 hours after seeding (expansion step I), the cell attachment was determined indirectly by counting the cells that did not adhere to the substrate. Values for attachment are

reported as mean percentage (relative to the number of inoculated cells) over the three donors, with standard deviation.

The AHACs' attachment tended to be higher on RGD (66±10 %) than on TCPS (56±21 %). On TCPS, a higher inter donor variability was observed than on RGD, as can be seen from the difference in standard deviation. Contrastingly, on PEG
(12±5 %) the cell attachment was fivefold lower as compared to on TCPS and RGD. These results are reflected by the phase contrast images C-E (Fig. 6.2) which showed a spread morphology for AHACs adherently growing on TCPS and RGD. On PEG in contrast, AHACs did not adhere. Instead, AHACs exhibited a round morphology, formed clusters and remained in suspension.

6.2.2 AHACs proliferate comparably on TCPS & RGD

Following attachment, AHACs were expanded on TCPS, RGD and PEG in two steps of 7 days each. The number of harvested cells from each expansion step was used to calculate the proliferation rate as doublings per day.

With a value of 0.56±0.04, the total proliferation rate of AHACS growing on RGD does not differ from that found in the TCPS-condition (0.62±0.06). Contrastingly on PEG, the total proliferation index (0.21±0.07) was more than two times lower as compared to on TCPS and RGD.
For all conditions, the proliferation index on the expansion step II was consistently increased by 31±8 % relative to expansion step I.

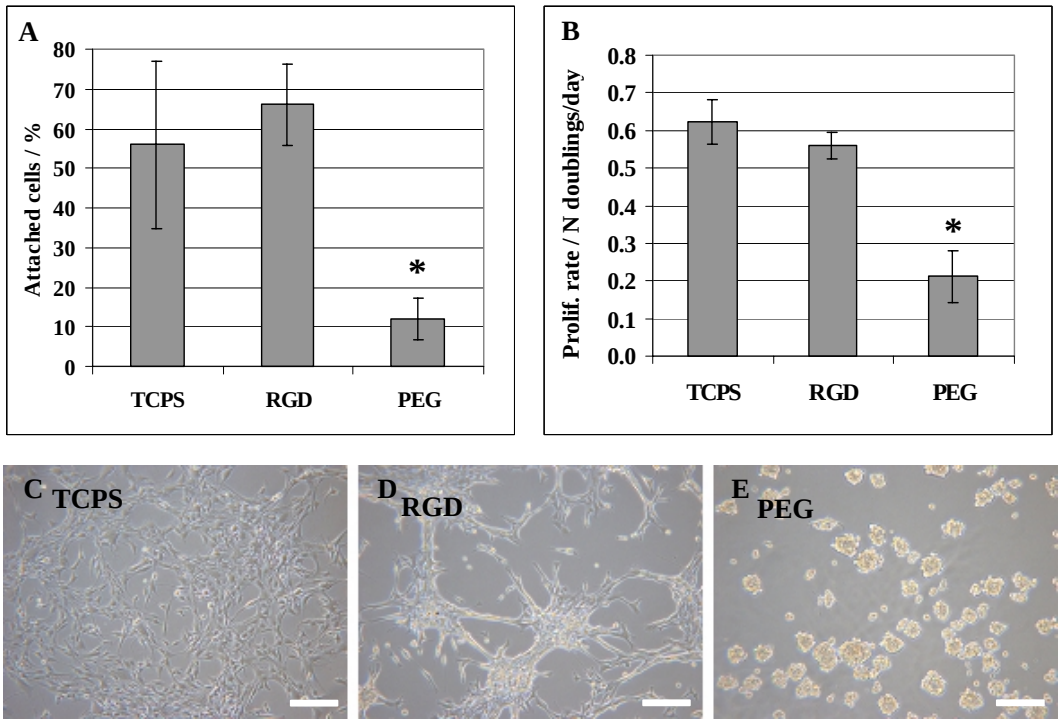

FIGURE 6.2 Attachment and proliferation of AHACs on TC, RGD and PEG. **A** The number of attached cells was determined indirectly by counting the floating cells in the supernatant (alive and dead) and subtracting them from the number of inoculated cells. The attachment is expressed as percentage of the number of inoculated cells. **B** The proliferation rate of AHACs is expressed as N doublings per day (during the two expansion steps). In graph A and B, the bars represent the mean value over the three donors on the corresponding surface, with error bars for the standard deviation. The asterisk indicates a significant difference *vs*. TC ($p = 0.05$). **C**, **D** and **F** show a phase contrast images of AHACs during expansion on the corresponding surface. Scale bars are 250 µm.

6.2.3 AHACs on RGD have greater perimeter than on TCPS

AHACs, frozen after expansion step II, were thawed and reseeded onto TCPS and RGD. The adherently grown AHACs, were fixed, permeabilized and labelled for actin and the nucleus prior to image acquisition with the confocal laser scanning microscope (CLSM). From randomly taken CLSM images all AHACs which were entirely contained within the frame were outlined, filled and their area and perimeter measured. These measurements were performed on 30 cells for each condition and used to determine the average shape factor $\phi_{A.}$.

On RGD, the values for ϕ_A on TCPS range from 0.128 to 0.189 whereas on RGD they are between 0.057 and 0.099. Thus, the average shape factor ϕ_A is 2 fold lower on RGD compared to that of AHACs expanded on TCPS. The average footprint area of AHACs ranged from 948 to 1450 μm^2 and did not significantly differ between neither TCPS and RGD nor between the three donors. Contrastingly, the AHACs average perimeter always differed between TCPS (330±22 μm) and RGD (424±27 μm) whereas on the same surface, there was no difference between the donors.

Throughout all conditions, ϕ_A did not exceed the value of 0.2, which indicates, that the AHACs tended to assume an ellipsoid and elongated morphology. This tendency is reflected by the selection of filled outlines (Fig. 6.3, image B). From each condition, two representative examples are displayed (TCPS: ϕ = 0.149 - 0.163, RGD ϕ = 0.076-0.081). The filled outlines also showed, that the thin, filopodia-like protrusions from the AHACs on RGD were present to a lower extent on AHACs expanded on TCPS. The main contribution to the increased perimeter of AHACs on RGD was found in the presence of these extensions.

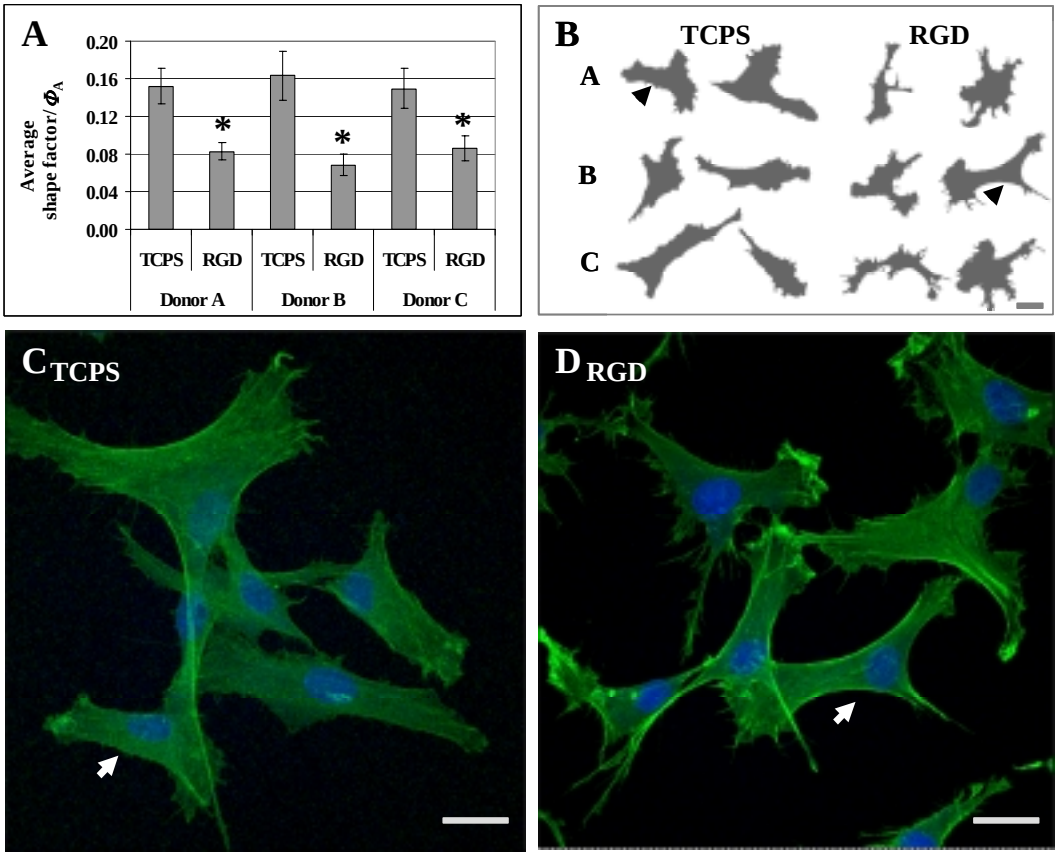

FIGURE 6.3 Morphology of AHACs on TC and RGD during expansion. **A** Graph, representing the values for the average shape factor (round: $\phi \approx 1$, thin thread-like: $\phi \approx 0$) of AHACs from donor A, B and C during expansion on TC and RGD.. The obtained values are presented as an average shape factor ϕ_A of 30 measurements. The asterisk indicates a significant difference *vs*. TC ($p = 0.05$). **B** Filled outlines of AHAC during expansion on TC and RGD (for donor A, B and C). These filled outlines were used to measure the AHACs' area and perimeter needed for the determination of the shape factor ϕ. From each condition, two representative examples are shown (TC: $\phi = 0.149$ - 0.163, RGD $\phi = 0.076$-0.081). The arrows point to the AHACs which were extracted from the CLSM images **C** & **D**, shown below. Actin stress fibres are displayed green and the nuclei in blue. Scale bars are 20 µm.

6.2.3.1 AHACs form more filopodia on RGD than on TCPS

The morphological difference of AHACs on TCPS and RGD (as expressed by the average shape factor ϕ_A) also becomes apparent by directly comparing the CLSM images. The actin stress fibres were labelled green whereas the nuclei were assigned the false colour blue. The nuclei were labelled to facilitate the distinction of overlapping cells.

On both TCPS and RGD, a homogenous fluorescence signal can be seen throughout the entire AHACs as actin appears to be mostly organized into fine filamentous structures. Only rarely, thicker actin bundles, as they are typical for stress fibres, occur. Regions of highest actin-signal intensities were located at the lamellipodia, as well as at the filopodia-like extensions. These extensions were the most distinctive morphological feature of AHACs adherently growing on RGD.

Remarkably, CLSM images from AHACs on RGD were consistently obtained with much lesser background fluorescence than on TCPS. As a consequence, most brilliant images were obtained from AHACs on RGD.

6.2.4 AHAC on TCPS and RGD are of comparable maximal height

AHACs during culture on TCPS and RGD were imaged by AFM. A custom built phase contrast microscope was used for tip positioning on the AHACs as well as to detect cell damage and tip contamination. To visualize the AHACs' topography and surface corrugations, height and deflection images presented in Fig. 6.4 were recorded from 40 µm scans in contact mode.

The average maximal height (measured from the height images) of AHACs expanded on TCPS (1.5±0.6 µm; n = 19) and RGD (1.5±0.3 µm; n = 4), was and thus was comparable in both conditions.
The deflection images of both AHACs growing on TCPS and RGD, revealed the presence of an interwoven, cytoskeletal network. This network was dominated by straight, fibre-like structures, of which some span the entire length of the AHACs. The fibres emerged in high density from cell corners and preferentially were oriented in parallel to the border of the cells.
Image H (Fig. 6.4), shows a branched processus extending more than 20 µm from the cell. Despite this structural feature, which was not seen on TCPS, there are no visible differences between the deflection images of AHACs during expansion on TCPS and RGD.

An image sequence was acquired to test, if scanning in contact mode would cause damage to the AHACs. The image sequence E, F, G (Fig. 6.4) was acquired over a time frame of 1h. Despite small rearrangements of the cytoskeletal network and the cell periphery, the overall morphology of the scanned AHAC remained nearly unaltered for up to 40 min (compare image E and F). Furthermore there were no signs of damage, such as cutting off or flipping over of lamellar portions.

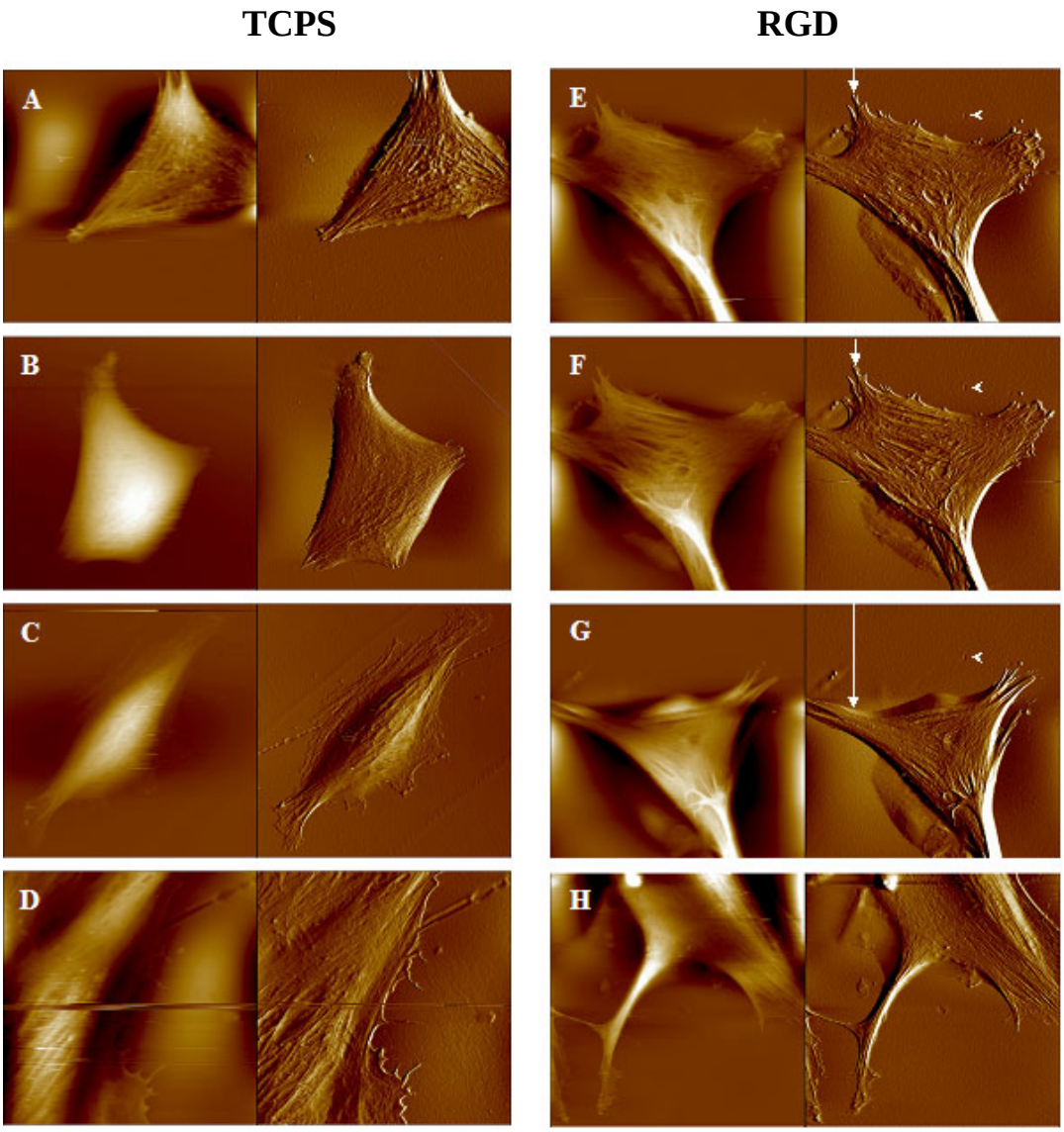

FIGURE 6.4 AFM height (left) and deflection (right) images from scans on AHACs during expansion on TCPS (left column) and RGD (right column). **A-C** Show 40 µm scans of AHACs adherent to TCPS. **D** Detail scan on upper right part of AHAC imaged in C, showing the lamellar region of the AHAC. Scan size: 20 µm. **E-G** 40 µm-scan image sequence of AHAC on RGD, acquired within 1 hour. The white arrow head points to the landmark used for the determination of the thermal drift, whereas the white, vertical arrow points to a motile extension of the AHAC. **H** AHAC with a ~20 µm long, branched processus. The z-ranges of the height (h:) and deflection (d:) images in nanometer are: A h: 2000, d: 20; B h: 2500, d: 11; C h: 2500, d: 10; D h: 1500, d: 8; E-G h: 2500, d: 12; H h: 2000, d: 10.

Contrastingly, obvious changes were visible in the last image of this sequence (image G). In detail, the motile extension of the AHAC (pointed out by a white, vertical arrow in the deflection images), retracted with an average speed of 3.2 nm/s. This value has been corrected for the drift, which was measured by referring to the position of a landmark (white arrow head in deflection images), relative to the border of the scanned image. This way, the thermal drift of the AFM was determined to be -1 µm/h in y-direction, whereas in x-direction there was no detectable positional change.
More clearly than on the deflection image, the height images E-G show a bright feature located in the lower corner of the scanned AHAC. To allow for a more plastic impression of the topology, the surface plot shown in Fig. 6.5 (image A) was generated from the height image G (Fig 6.4). Thereon, an extension of an AHAC from outside the scan range is visible as a brightly colored crest, which partially covers posterior aspects of the imaged AHAC. In a section analysis (Fig. 6.5 image B & C), a step height of 0.5 µm was found for this crest which resides on a 0.7 µm thick portion of the imaged AHAC.

Furthermore, the average height of the lamellar region was determined to be 0.23 µm by a bearing analysis. This function is available in the Digital Instruments AFM software and allows to analyze the height distribution in a selected image area. In the section analysis, the height of the, peak pointed out by the black arrow head in Fig. 6.5 (image B & C) represents the average peak height within the lamellar region as it was found by the bearing analysis.

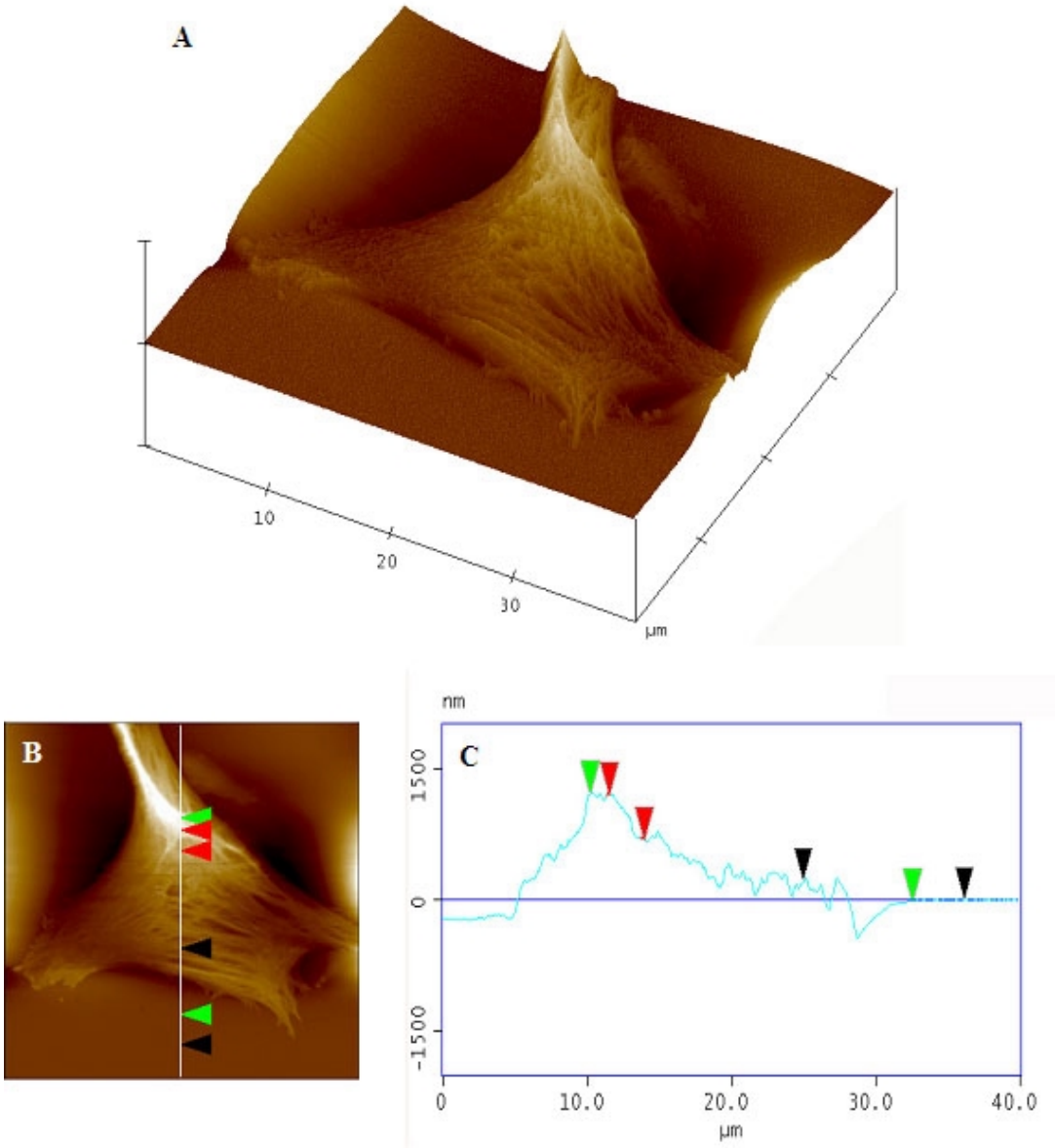

FIGURE 6.5 AFM surface plot and section analysis of an AHAC on RGD (scan size 40 µm). **A** Shows a surface plot of the AHAC presented in image F of Fig. 6.4 to allow for a more plastic impression of the topology. An extension of an AHAC from outside the scan range is visible as a brightly coloured crest that partially covers posterior aspects of the imaged AHAC. **B** Height image of an AHAC on RGD, with arrow heads indicating the position of the different height measurements along the chosen section (white line). The green and the black arrow positioned on the substrate (equally brown coloured area surrounding the cell) were taken as zero height. **C** By section analysis, the measured vertical distance between the paired arrow heads was : green: 1.24 µm, red: 514 nm; black: 215 nm

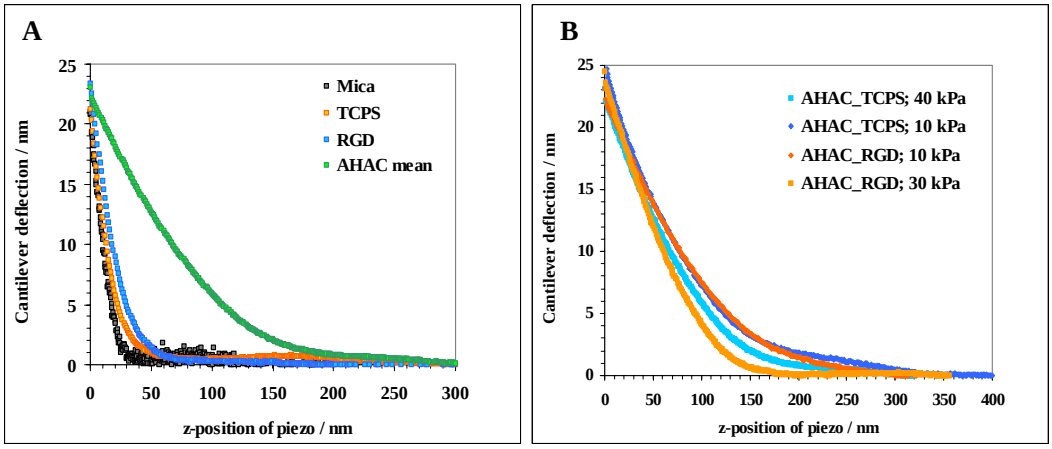

FIGURE 6.6 AFM load-displacement curves on Mica/TCPS/RGD and AHACs during expansion on TCPS and RGD. **A** Qualitative comparison of different load-displacement curves. Mica as an infinitively stiff substrate was used to calibrate the cantilever sensitivity and was compared with TCPS and RGD. AHAC mean represents the average of the four curves shown in **B** Load-displacement curves from four individual cells during expansion on TCPS (n = 2) and RGD (n = 2). The legend shows the approximate elastic modulus for each curve.

6.2.4.1 On RGD & TCPS AHACs are comparably elastic

In addition to imaging, the elasticity of AHACs was determined in a preliminary experiment, using the AFM as a nanoindenter. On 5 µm scans in the lamellar region, 256 force curves were recorded, using a soft cantilever (0.03 N/m). From this data set, the average force curve was calculated and the elastic modulus approximated thereof.

The calibration curve on mica had a slope of 45° as it is expected for an infinitively stiff substrate. While the force curve on TCPS was almost superimposable with that on mica, the force curve on RGD showed a slight reduction in slope. Contrastingly, on AHACs the slope of the force curves was markedly reduced, which revealed the relative softness of living cells. Still, the range of the approximated elastic modulus found for AHACs on RGD (10-30 kPa, n = 2) did not differ from that of AHACs on TCPS (10-40 kPa, n=2).

6.2.5 AHACs motility tends to be higher on TCPS

Observation by AFM showed, that AHAC morphology can be of dynamic nature. Moreover, CLSM revealed morphological features which point to a distinctive AHAC motility on RGD. Thus, time-lapse microscopy was performed to further analyze the effect of TCPS and RGD on AHACs' motility. AHACs from donor B and C were imaged every 5 min. over a time span of 7 hours, starting 24 hours *post* inoculation. From each resulting image series, randomly chosen AHACs ($n \geq 100$) were manually tracked with Image Pro. From the total length of the trajectories, the average speed was calculated in nm/s.

The distribution of average speed ranged from AHACs which remained nearly static to AHACs that were moving as fast as 16.5 nm/s, which was approximately 4 times faster than the mean speed found throughout all the conditions. Assuming a normal distribution for the average speed measurements in all the conditions but donor B/RGD, the mean speed was calculated. For donor B/RGD, where a big fraction of the AHACs showed low motility, the median was determined. The mean speed is presented with a two sided confidence interval of 95%.

With 4.9±0.5 nm/s the AHACs of donor B were approximately 30% faster on TCPS than on RGD, where their mean speed was 3.5±0.3 nm/s. Though not significant, for donor C, AHACs still tended to be faster on TCPS (4.3±0.3 nm/s) than on RGD (4.0±0.2 nm/s).

The phase contrast images for donor C show, that the initial cell density was the same on TCPS and RGD. Additionally, based on the orientation of the trajectories, the motion of the AHACs showed no net direction but appeared to be fully random.

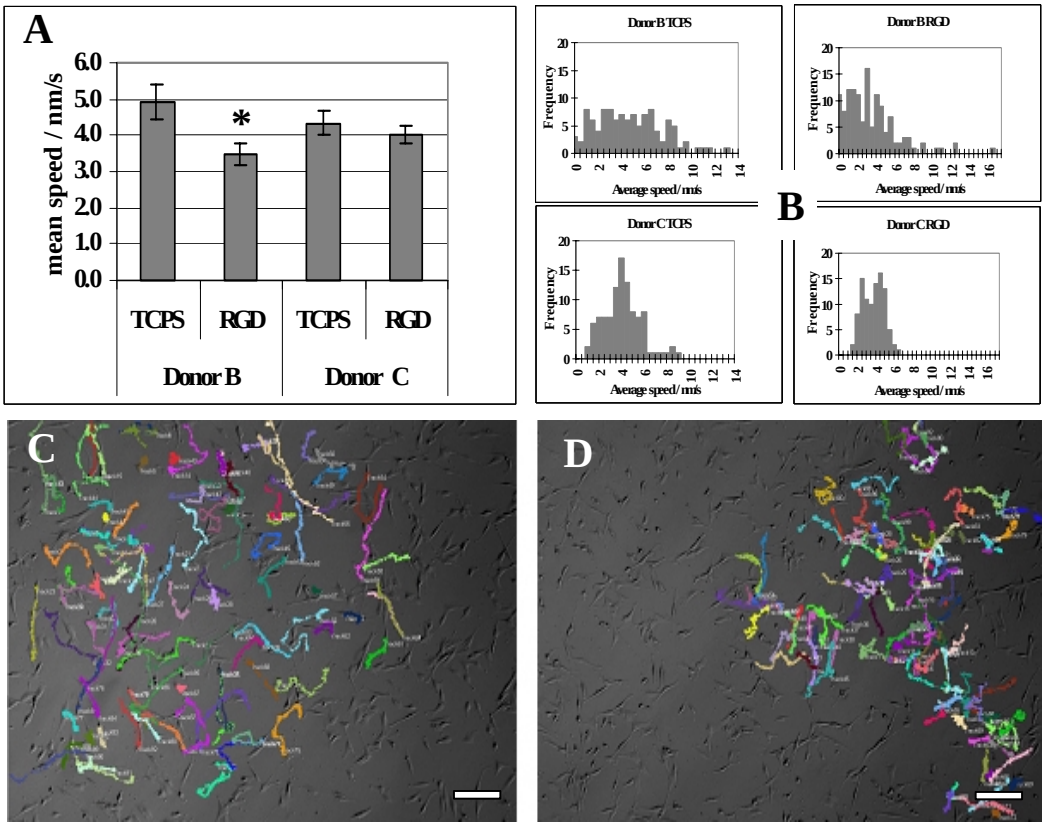

FIGURE 6.7 Motility of AHACs on TCPS and RGD. **A** The bars represent the mean speed in nm/s of AHACs from donor **B** and C on TCPS and RGD. For each condition, AHACs ($n \geq 100$) were tracked over a time span of 7 hours by time lapse phase-contrast microscopy. The asterisk indicates a significant difference *vs*. TCPS ($p = 0.05$). B represents the distribution of the AHACs' (from donor B and C) average speed on TCPS and RGD. **C** shows a phase contrast image of the AHACs from donor C, 24 hours post inoculation on TCPS, whereas on **D** the surface is RGD. The randomly coloured trajectories of the manually tracked AHACs are presented in overlay of the phase contrast images. Scale bars are 200 µm.

6.2.6 During AHAC expansion Coll II mRNA levels were higher on RGD

AHACs harvested at the end of expansion step II on TCPS, RGD and PEG were analysed for their mRNA expression levels of the chondrogenic markers collagen I, II and X by real-time quantitative PCR. The amount of mRNA was normalized to the quantity of the housekeeping gene 18-S RNA and the expression level reported as fold up-regulation relative to the corresponding TCPS condition.

As shown in Fig. 6.8, AHACs expanded on RGD have five-fold increased collagen II mRNA expression while the level for Collagen I mRNA remained unaltered. Due to the high inter-donor variability, no significance was found for the 12-fold up-regulation of collagen X mRNA.

On PEG, the collagen II mRNA up-regulation by more than one order of magnitude coincided with a collagen X mRNA expression level that was increased by nearly two orders of magnitude. The expression level of collagen I mRNA did not change.

6.3 *POST* EXPANSION EFFECT OF TCPS, RGD & PEG ON THE CHONDROGENIC CAPACITY OF AHACs

AHACs expanded on TCPS, RGD and PEG were pelleted and cultured in chondrogenic medium for two weeks to investigate the influence of RGD on their chondrogenicity. The obtained pellets were analyzed biochemically histologically.

Two entire pellets were used for each analysis and condition except for PEG. As on PEG, the proliferation rate of AHACs was markedly reduced, the number of cells obtained from donor A was to low for pellet preparation. Consequently, for donor B and C the area of the expansion surface and the initial number of cells taken into expansion on PEG was increased four-fold. Still, the number of cells after expansion step II was not sufficient. Thus, instead of six, three pellets (one pellet for each analysis) could be prepared from donor B and five for donor C (mRNA: 2; biochemistry:2; histology: 1).

6.3.1 AHAC expansion mRNA expression-pattern was not reflected in pellets

Upon termination of the pellet culture, the mRNA expression level of collagen I, II and X was analyzed by quantitative RT-PCR and expressed as fold up-regulation vs. TCPS.

The up-regulation of collagen II mRNA during the expansion of AHACs on both, RGD and PEG was not reflected in the pellet culture. Only for collagen X mRNA a slight up-regulation (1.7-fold) was found. Due to the high interdonor variability, no significance was found for the highest up-regulation, which was obtained for collagen II mRNA on PEG.

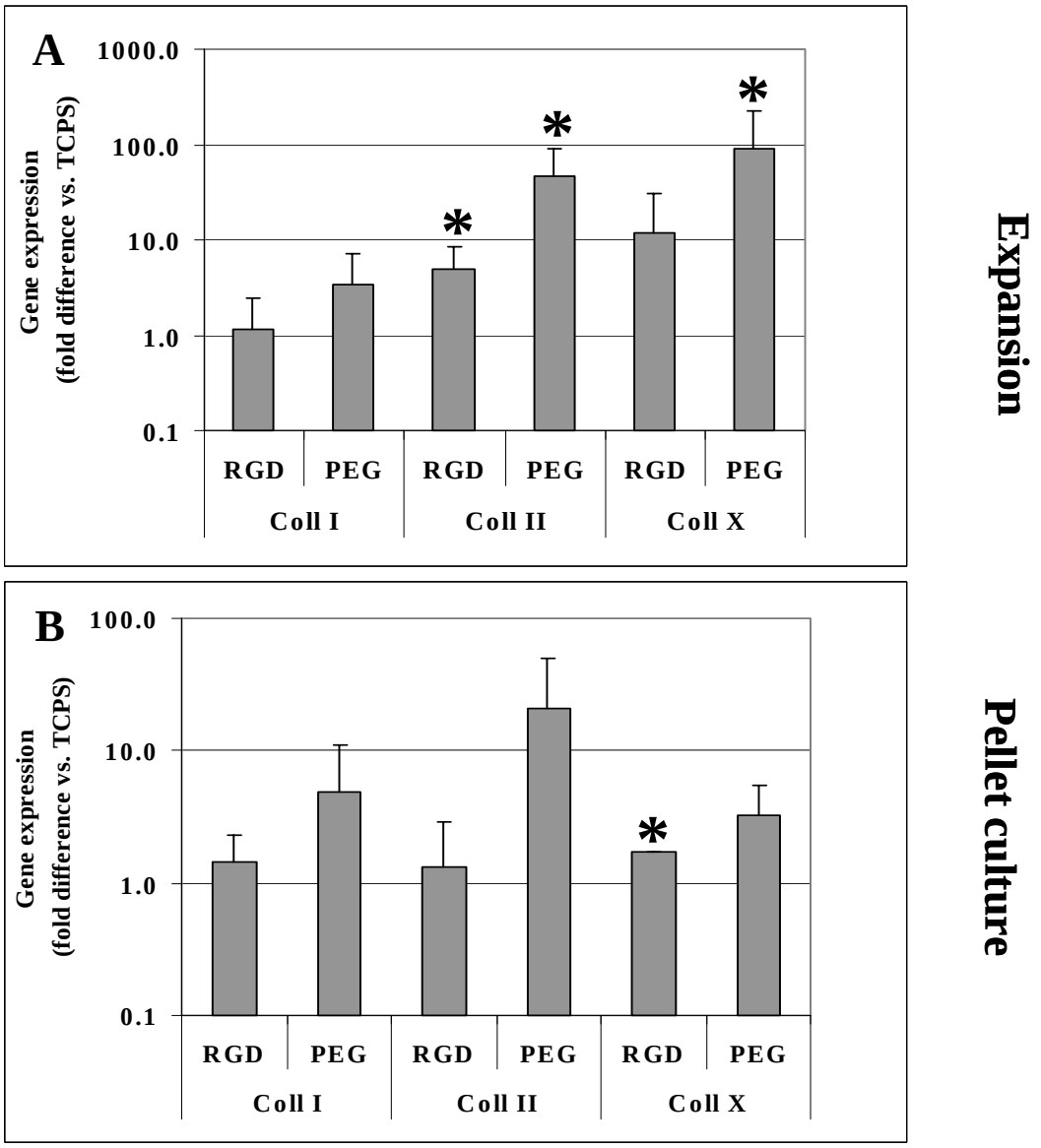

FIGURE 6.8 Collagen I, II and X mRNA expression levels of AHACs during expansion and in subsequent pellet culture. **A** mRNA expression level of AHACs during expansion (at the end of expansion step II) on the surfaces TCPS, RGD and PEG. **B** m RNA expression of AHACs after two weeks of pellet culture in chondrogenic medium. TCPS, RGD and PEG indicate the surface on which the AHACs were expanded prior to pelleting. The bars represent the mean of the n donors (RGD: n = 3, PEG: n = 2) with a positive error bar for the standard deviation. The values express the fold difference resulting from the surfaces RGD and PEG vs. TCPS. The asterisk indicates a significant difference *vs*. TCPS (p = 0.05).

6.3.2 Pellets from AHACs expanded on RGD contained more GAG/DNA

Pellets from AHACs expanded on RGD showed a slightly but consistently higher GAG/DNA (5.76±0.5 µg/µg) accumulation than the pellets from the TCPS condition. The highest level of GAG/DNA (7 µg/µg) was found for the pellet formed with AHACs expanded on PEG (donor B).

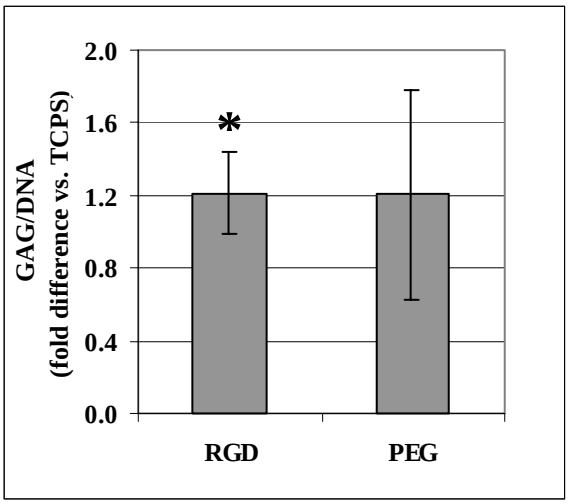

FIGURE 6.9 GAG/DNA in pellets generated from AHACs expanded on RGD (n = 3) and PEG (n = 2). The bars represent the mean value of n donors relative to TCPS with error bars indicating the standard deviation. The asterisk indicates a significant difference *vs*. TCPS (p = 0.05)

Almost no differences in the staining for GAG could be seen between the conditions TCPS and RGD. The highest intensity for GAG staining was observed in pellets generated with AHACs expanded on PEG.

Despite of the pellet from the PEG condition of donor C, the intensity of the Safranin O staining confirmed the results for sulphated GAG per DNA.

Pellet sections immunohistochemically labeled for collagen only showed small differences between the conditions TCPS and RGD. PEG (donor C), showed the highest intensity for collagen II These results reflect the finding for Collagen II mRNA

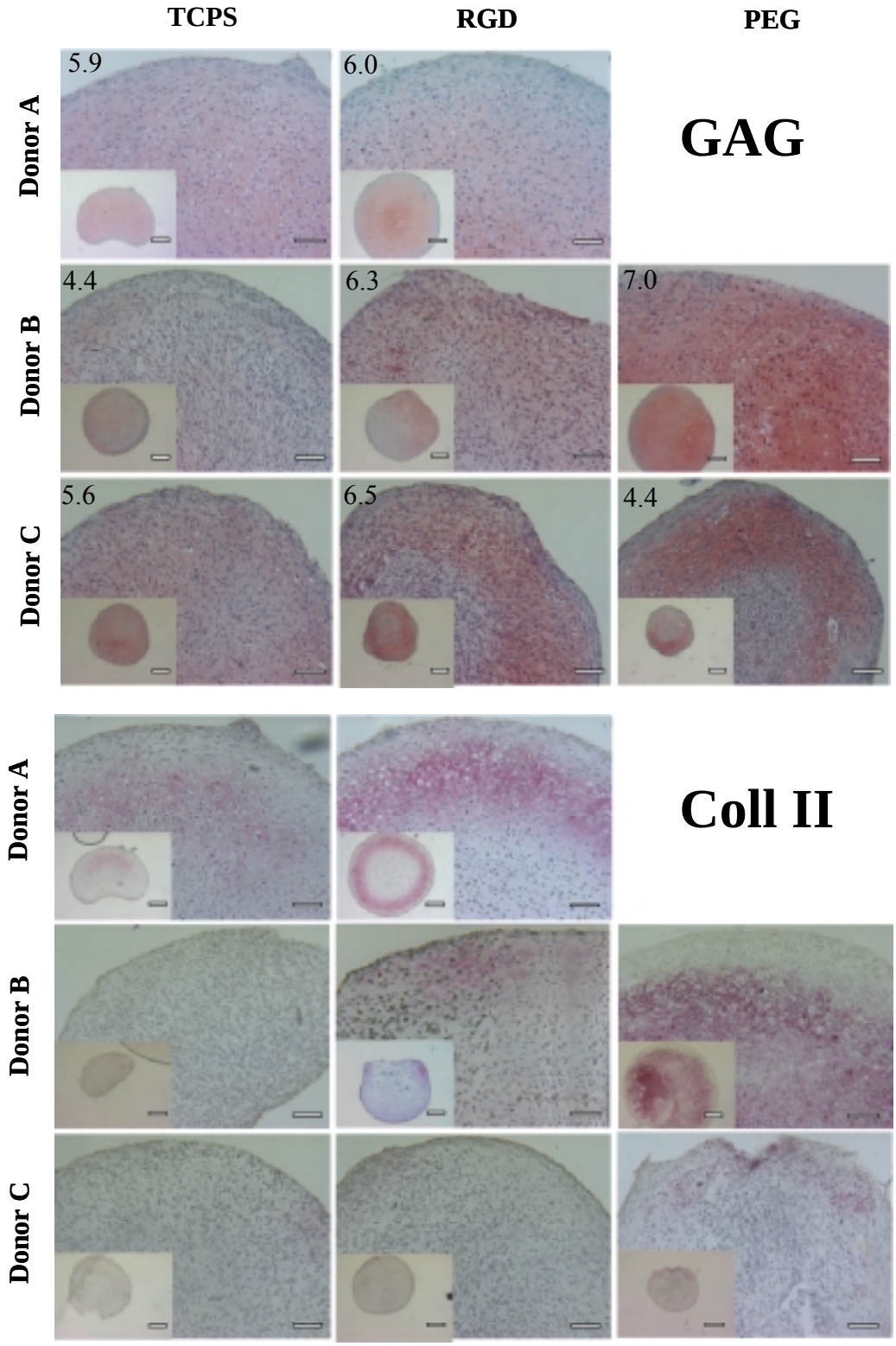

FIGURE 6.10 Histology of pellets generated from AHACs expanded on TCPS, RGD and PEG. The upper half of the figure shows pellet sections stained red for GAG with Safranin O. The number in the upper left of each image shows the value for accumulated GAG/DNA (µg/ug). The lower half of this figure shows pellet sections which were immunohistochemically labelled red for collagen II (Coll II). Representative sections are displayed for each donor and condition. Scale bars: 50 µm. As an overview, the insets present entire pellet sections. Scale bars are 500 µm.

7 DISCUSSION & CONCLUSIONS

The effect of the synthetic, cell-adhesion mediating PLL-g-PEG/PEG-g-RGD surface on AHACs during and *post* expansion was investigated using complementary techniques.

7.1 SURFACE CHARACTERIZATION

Tissue culture treated polystyrene (TCPS) is a commonly used standard material for *in vitro* culture of adherently growing cells. Its surface presents negatively charged functional groups, onto which serum proteins can adsorb. Fibronectin, which is a soluble serum protein, is one of many known ECM proteins, that mediates specific interaction of cells to surfaces via cell integrin receptors (Garcia and Boettiger, 1999). As such, cell adhesion is not mediated by TCPS *per se* but by its serum protein adlayer. The formation of such an adlayer was qualitatively shown by the AFM surface topology analysis of TCPS, before and after exposure to serum containing culture medium. The relatively amorphous pattern could be explained by a wide variety of serum proteins which can compete with fibronectin for binding sites on TCPS (Koenig et al., 2002).

Adsorption of the RGD-functionalized PLL-*g*-PEG copolymer was also visualized by AFM. The fact, that the topology did not markedly differ from that of the untreated Thermanox® surface is most likely explained by the presence of a very homogenous coating. In fact, PLL-*g*-PEG adsorbed to negatively charged surfaces are known to build a brush like monolayer in aqueous solution (Heuberger et al., 2005).

Another indicator, that the RGD-functionalized polymer uniformly coats the substrate becomes apparent when comparing the CLSM images from AHACs on TCPS and RGD. On TCPS, background signals originating from non-specifically adsorbed fluorescent probes were always present, whereas on RGD they were not. This effect can be attributed to poly (ethylene glycol). The pegylated surface builds a brush-like border that prevents non-specific protein adsorption (Elbert and Hubbell J.A., 1996). Therefore, fluorescent probes can not cross-react with or non-specifically adsorb to the surface via serum proteins and can be rinsed off the surface during the washing steps.

7.2 AHAC ATTACHMENT AND PROLIFERATION

Cell attachment and proliferation, as it occured on TCPS, can be reproduced on RGD. Where the RGD-sequence containing dodecapeptide was not present, as it is the case on PEG, cell attachment was drastically decreased. Furthermore on non-functionalized PEG, AHACs did not spread, assumed a round morphology and remained clustered in suspension. Moreover, they proliferated at a markedly lower rate than on TCPS and RGD. Therefore, cell attachment, spreading and proliferation appeared to be specifically induced by the RGD-functionalized copolymer PLL-g-PEG/PEG-RGD. These findings are in line with results reported for human dermal fibroblasts (Schuler et al., 2006).

7.3 AHAC MORPHOLOGY DURING EXPANSION

Whereas the measured footprint area of AHACs did not differ on TCPS and RGD, the perimeter was consistently increased on RGD, which is expressed by the reduced shape factor. The increase in perimeter can mainly be contributed to the filopodia-like extensions. They were seen as a distinctive morphological feature of AHACs on RGD. Protrusive structures are known to occur at the

leading edge of motile cells. They are highly dynamic and contain dense arrays of actin filaments. The simplest protrusive structures are filopodia, thin cylinders that can extend tens of microns from the main cortex (Mitchison and Cramer, 1996). Based on this morphological information, AHACs were expected to be more motile on RGD than on TCPS. Time-lapse phase contrast microscopy revealed small, significant changes but of opposite trend. As AHACs on RGD tended to be of lower motility than on TCPS, their distinctive protrusive structures are more likely to be retracting tails, which from RGD do not de-adhere as well as from TCPS. This interpretation also finds support by publications, that report on the inverse relationship between motility and adhesion strength (Tziampazis et al., 2000).

Only few AHACs on RGD were scanned by AFM. In contrast to the images obtained by CLSM, the distinct protrusive structures were not as dominant. This raises the question, if the morphology analysis by CLSM was affected by artefacts (e.g. damage of surface) introduced during sample preparation.

To test, whether these protrusions are retracting tails or sample preparation artefacts, AHACs on RGD should be further analyzed by optical time-lapse microscopy at high magnification. This could involve the use of fluorescent vital probes to enhance the contrast of the cell membrane.

7.4 AFM SAMPLE PREPARATION

A method was developed, which allowed the use of tissue culture plastic as a substrate with the custom built phase contrast set-up for the multimode AFM.

In a first approach, round lamellae were punched out of tissue culture treated petri dishes with a stencil, as the intention was to use the same substrate material for AFM of AHACs as during the expansion. Due to their thickness, the petri dishes would also have been ideal to allow for high substrate rigidity. However, the punching induced high tensions to the polystyrene which, as a consequence started to splinter. Lamellae from Thermanox®, as an alternative, were easy to punch out with a stencil, due to its low thickness (0.17 mm). These lamellae were then glued onto a supportive glass lamella (thickness: 0.3 mm) with epoxy glue. These compound lamellae were of sufficient optical quality to allow for the visualization of AHACs in the phase contrast set-up. Furthermore, these compound lamellae, glued into the PTFE ring of phase contrast-sample-holder with epoxy glue, remained firmly in place and allowed the AFM to be driven at high integral and proportional gains. This is of high importance, since low gains have been observed to be related to both, insufficient immobilization of the sample-support and to insufficient substrate rigidity. As consequence of low gains, the probe can not properly follow the sample topography, starts to oscillate and even causes damage, especially to soft samples as i.e. cells. These damages can be seen as cutting off or flapping over of cell-portions as well as the ripping off of entire cells.

7.5 ELASTICITY OF AHACs

Using the AFM as a nanoindenter, AHACs on RGD and TCPS showed to be of comparable elasticity. Although the elasticity of each AHAC was determined from a data set that was large enough to allow for statistical analysis, the finding remained of preliminary character. This was mainly due to the limited number of measurements.

From the averaged force curves it can be seen, that the onset of tip-sample contact is difficult to detect. This is because soft biological samples, compared to hard materials are 4-6 orders-of-magnitude lower in stiffness and can have a more irregular topology (Stolz et al., 2004). In the elasticity measurements of AHACs, the maximal penetration depth was around 120 nm. Given an average height of 0.2 μm for the indented lamellar region, the Bueckle's indentation depth limit was clearly exceeded (Bueckle, 1973;Persch et al., 1994). Thus, stiffness contributions from the substrate are likely . Nevertheless, the range of elasticity values for AHACs found in this thesis was matching that found in the literature (Bao and Suresh, 2003).
Further elasticity measurements of AHACs on both, RGD and TCPS are needed to consolidate this preliminary finding.

7.6 AHAC PHENOTYPE & CONDROGENIC CAPACITY

High interdonor variability was observed for the mRNA expression levels of all three chondrogenic markers. This problem could be overcome by increasing the number of samples. Yet, the number of donors is limited. Thus in this thesis, the number of donors was limited to 3 and the effect of RGD relative to TCPS compared intradonor-wise by using a paired, non-parametrical statistical test (Mann-Whitney).

During expansion, the up-regulation of collagen II mRNA indicated a better maintainance of the chondrogenic phenotype of AHACs expanded on RGD as compared to on TCPS. On PEG this effect was even more pronounced but there, the increased collagen X mRNA expression is a sign, that the AHACs shifted towards a hypertrophic phenotype. As described above, AHACs could not attach to PEG and thus remained suspended in the culture medium, where they formed clusters. This *in vitro* condition, in which AHACs are cultured in suspension is known to promote the onset of a hypertrophic phenotype in a limited fraction of clusters (Stephens et al., 1992). Based on gene expression analysis of culture-expanded AHACs, a model of chondrocyte development has been proposed, wherein hypertrophic and articular chondrocytes belong to separate lineages (Binette et al., 1998).

The mRNA expression level of AHACs during expansion was not reflected in pellet culture. The only significant up-regulation was found for collagen X on RGD. However, this was not considered to be biologically relevant.

As on PEG the proliferation of AHACs was markedly reduced, only for two donors, pellets could be generated. Due to the combination of the interdonor variability, with the reduced number of samples, the strongest up-regulation was not detected to be significant. Still, pellets generated from AHACs (Donor B)

expanded on PEG consistently showed to contain chondrocytes of highest chondrogenic capacity. Although this is remarkable, the chondrogenic capacity of AHACs expanded on PEG remains unclear. Thus, the chondrogenic assay for the PEG condition should be repeated with a higher number of samples.

The AHACs expanded on RGD did not differ in their chondrogenic capacity from those expanded on TCPS. Thus, RGD seemed to be able to mimick the characteristics of TCPS, which influence the *post* expansion chondrogenic capacity of AHACs

7.7 Conclusion

In comparison to TCPS, AHACs during expansion on the RGD-modified surface showed a higher expression of the chondrogenic marker collagen II mRNA. Furthermore on RGD, AHACs formed more filopodia but tended to be slightly less motile than on TCPS. In the subsequent *in vitro* chondrogenic assay, however the found differences for collagen II mRNA were not reflected. Furthermore, the formed, cartilaginous matrix of the pellets generated from AHACs expanded on RGD did not differ from that of pellets obtained from AHACs expanded on TCPS.

The surface-cell interaction of AHACs, as it appears to be specifically mediated by the dodecapeptide of the RGD-functionalized PLL-*g*-PEG, is the prerequisite for cell attachment and subsequent proliferation. Moreover it also seems, that the interaction of the integrins with the RGD-functionalized surface supports the chondrogenic phenotype during expansion of AHACs in a 2D layer. However, this effect does not seem to be sustained in the absence of the RGD-modified surface in the subsequent pellet culture. Thus, ongoing work should include RGD-modified surfaces in a 3D *in vitro* chondrogenic assay.

8 ACKNOWLEDGMENTS

Thanks to:

…Marcus Textor, Ueli Aebi, Ivan Martin and Samuele Tosatti for their support and open minded attitude towards my ideas.

…the company F. Hoffmann-La Roche AG and the ICFS of the University Hospital Basel, for the scholarship. It has greatly helped me focussing on my project.

…Andrea Barbero for all his advice and substantial support. Mille grazie!

…Martin Schuler, for synthesizing the polymers, his support and patience.

…Francine Wolf, for her tremendous help with the pellet analysis, merci!

…to Marija Plodinec, Martin Stolz and Riccardo Gottardi for introducing me to the secrets of AFM force measurements.

…Simon Ströbel for contributing his ideas, and enriching discussions

…to Annina, for challenging me to be more efficient. Thank you for being in my life!

9 REFERENCES

1. Bao,G. and S.Suresh. 2003. Cell and Molecular Mechanics of Biological Materials. *Nature Materials* 2:715-725.

2. Barbero,A., S.Ploegert, M.Heberer, and I.Martin. 2003. Plasticity of Clonal Populations of Dedifferentiated Adult Human Articular Chondrocytes. *Arthritis & Rheumatism* 48:1315-1325.

3. Barbero,A., S.Grogan, D.Schafer, M.Heberer, P.Mainil-Varlet, and I.Martin. 2004. Age related changes in human articular chondrocyte yield, proliferation and post-expansion chondrogenic capacity. *Osteoarthritis and Cartilage* 12:476-484.

4. Binette,F., D.P.McQuarid, D.R.Haudenschild, P.C.Yaeger, J.M.McPherson, and R.Tubo. 1998. Expresseion of a Stable Articular Cartilage Phenotype without Evidence of Hypertrophy by Adult Human Articular Chondrocytes *in vitro*. *J Orthop Res* 16:207-216.

5. Bueckle,H. 1973. The Science of Hardness Testing and its Research Applications. American Society for Metals, Materials Park, Ohio.

6. Elbert,D.L. and Hubbell J.A. 1996. Surface Treatments of Polymers for Biocompatibility. *Annual Review of Materials* 26:365-370.

7. Farndale R.W., D.J.Buttle, and Barrett A.J. 1986. Improved Quantitation and Discrimination of Sulfphated Glycosaminoglycans by use of Dimethylene Blue. *Biochim Biophys Acta* 883:173-177.

8. Garcia,A.J. and D.Boettiger. 1999. Integrin-fibronectin Interactions at the Cell-material Interface: Initial Integrin Bining and Signalling. *Biomaterials* 20:2427-2433.

9. Garciadiego-Cázares,D., C.Rosales, M.Hatoh, and J.Chimal-Monroy. 2004. Coordination of chondrocyte differentiation and joint formation by á5â1 integrin in the developing appendicular skeleton. *Development* 131:4735-4742.

10. Grimmer,J.F., C.B.Gunnlaugsson, E.Alsberg, H.S.Murphy, H.J.Kong, D.J.Mooney, and R.A.Weatherly. 2004. Tracheal Reconstruction Using Tissue-Engineered Cartilage. *Arch Otolaryngol Head Neck Surg* 130:1191-1196.

11. Grogan S.P., Rieser F., Winkelmann V., Berardi S., and Mainil-Varlet P. 2003. Static, Closed and Scaffold-Free Bioreactor System that Permits Chondrogenesis *in vitro*. *Osteoarthritis Cart* 11:403-411.

12. Hersel,U., C.Dahmen, and H.Kessler. 2003. RGD Modified Polymers:Biomaterials for Stimulated Cell Adhesion and Beyond. *Biomaterials* 24:4385-4415.

13. Hersel,U., C.Dahmen, and H.Kessler. 2006. RGD Modified Polymers:Biomaterials for Stimulated Cell Adhesion and Beyond. *Biomaterials* 24:4385-4415.

14. Heuberger,M., T.Drobek, and Spencer N.D. 2005. Interaction Forces and Morphology of a Protein-Restitant Poly(ethylene glycol) Layer. *Biophys J.* 88:495-504.

15. Hollander,A.P., T.F.Heathfield, C.Webber, Y.B.R.Iwata, and A.Rorabeck. 1994. Increased Damage to Type II Collagen in Osteoarthritic Articular Cartilage Detected by a New Immunoassay. *J Clin Invest* 93:1722-1732.

16. Hsu,S., S.Whu, S.Hsieh, C.Tsai, D.Chen, and T.Tan. 2004. Evaluation of Chitosan-alginate-hyaluronate Complexes Modified by an RGD-containing Protein as Tissue-engineering Scaffold for Cartilage Repair. *Artificial Organs* 8:693-703.

17. Huang,N.P., R.Michel, J.Voros, M.Textor, R.Hofer, and A.Rossi. 2000. Poly(L-lysine)-*g*-poly(ethylene glycol) Layers on Metal Oxide Surfaces: Surface-analytical Characterization and Resistance to Serum and Fibrinogen Adsorption. *Langmuir* 2:489-498.

18. Jakob,M., O.Demarteau, D.Schafer, B.Hintermann, W.Dick, and M.Heberer. 2001. Specific Growth Factors During the Expansion and Redifferentiation of Adult Human Articular Chnodrocytes Enhance Chondrogenesis and Cartilaginous Tissue Formation *in vitro*. *J Cell Biochem* 81:368-377.

19. Ji,J., H.Zhu, and J.Shen. 2004. Surface Tailoring of Poly(DL-lactic acid) by Ligand-tethered amphiphilic Polymer for Promoting Chondrocyte Attachment and Growth. *Biomaterials* 25:1859-1867.

20. Kenausis,G.L., D.L.Elbert, N.P.Huang, R.Hofer, and L.Ruiz-Taylor. 2000. Poly(L-lysine)-*g*-poly(ethylene glycol) Layers on Metal Oxide Surfaces: Attachment Mechanism and Effects of Polymer Architecture on Resistance to Protein Adsorption. *J Phys Chem B* 14:3298-3309.

21. Kim,M.R., J.H.Jeong, and T.G.Park. 2002. Swelling Induced Detachment of Chondrocytes Using RGD-Modified Poly(*N*-isopropylacrylamide) Hydrogel Beads. *Biotechnol. Prog.* 18:495-500.

22. Koenig,A.L., V.Gambillara, and D.W.Grainger. 2002. Correlating Fibronectin Adsorption with Endothelieal Cell Adhesion and Signaling on Polymer Substrates. *J Biomed Mater Res 64*:20-37.

23. Lebaron,R.G. and K.A.Athanasiou. 2000. Extracellular Matrix Cell Adhesion Peptides: Functional Applications in Orthopaedic Materials. *Tissue Eng.* 6:85-103.

24. Lutolf,M.P. and J.A.Hubbell. 2005. Synthetic Biomaterials as Instructive Extracellular Microenvironments for Morphogenesis in Tissue Engineering. *Nat. Biotechnol.* 23:47-55.

25. Martin,I. and O.Frank. 2003. Real-time Quantitative RT-PCR Assays. *In* Biopolymer Methods in Tissue Engineering. Humana Press, Totowa, NJ, USA. 231-8.

26. Martin,I., M.Jakob, D.Schafer, W.Dick, G.Spagnoli, and M.Heberer. 2001. Quantitative analysis of Gene Expression in Human Articular Cartilage from Normal and Osteoarthritic Joints. *Osteoarthritis Cart* 9:112-118.

27. Mitchison,T.J. and L.P.Cramer. 1996. Actin-Based Cell Motility and Cell Locomotion. *Cell* 84:371-379.

28. Morra,M. 2000. On the Molecular Basis of Fouling Resistance. *J Biomat Sci-Polym* 6:547-569.

29. Persch,G., C.Born, and B.Utesch. 1994. Nano-hardness Investigations of Thin Films by Atomic Force Microscope. *Microelec. Eng.* 24:113-121.

30. Pierschbacher,E. and E.Ruoslahti. 1984. Cell Attachment Activity of Fibronectin can be Duplicated by Small Synthetic Fragments of the Molecule. *Nature* 309:30-33.

31. Rotsch,C., F.Braet, E.Wisse, and M.Radmacher. 1997. AFM Imaging and Elasticity Measurements on Living Rat Macrophages. *Cell Biology International* 11:685-696.

32. Ruoslahti,E. and M.D.Pierschbacher. 1997. New Perspectives in Cell Adhesion: RGD and Integrins. *Science* 238:491-497.

33. Schuler,M., G.R.Owen, D.W.Hamilton, M.de Wild, M.Textor, and S.Tosatti. 2006. Biomimetic Modification of Titanium Dental Implant Model Surfaces Using the RGDSP-Peptide Sequence: A Cell Morphology Study. S*ubmitted to Biomaterials*.

34. Sittinger,M., C.Perka, O.Schultz, T.Haupl, and G.R.Burmester. 1999. Joint Cartilage Regeneration by Tissue Engineering. *Z Rheumatol* 58:130-135.

35. Stamenovic´,D. and N.Wang. 2000. Cellular Responses to Mechanical Stress. Invited Review: Engineering Approaches to Cytoskeletal Mechanics. *J Appl. Physiol.* 89:2085-2090.

36. Stephens,M., Kwan A.P., and M.T.A.C.W.Bayliss. 1992. Human Articular Chondrocytes Initiate Alkaline Phosphatase and Type X Collagen Synthesis in Suspension Culture. *J Cell Sci* 103:1111-1116.

37. Stolz,M., R.Raiteri, A.U.Daniels, VanLandigham M.R., W.Baschong, and U.Aebi. 2004. Dynamic Elastic Modulus of Porcine Articular Cartilage Determined at Two Different Levels of Tissue Organization by Indentation-Type Atomic Force Microscopy. *Biopyhsical Journal* 86:1-15.

38. Tosatti, Samuele. Functionalized Titanium Surfaces For Biomedical Applications: Physico-chemical Characterization and Biological *in vitro* evaluation. 2005. Ref Type: Thesis/Dissertation

39. Tossati,S., S.M.De Paul, A.Askendal, S.VandeVondele, J.A.Hubbell, and P.Tengvall. 2003. Peptide Functionalized Poly(L-Lysine)-*g*-poly(ethylene glycol) on Titanium: Resistance to Protein Adsorption in Full Heparinized Human Bloood Plasma. *Biomaterials* 27:4949-4985.

40. Tziampazis,E., J.Kohn, and Moghe P.V. 2000. PEG-variant Biomaterials as Selectively Adhesive Proteins Templates: Model Surfaces for Controlled Cell Adhesion and Migration. *Biomaterials* 21:511-520.

41. van der Flier,A. and A.Sonnenberg. 2001. Functions and Interactions of Integrins. *Cell Tissue Res* 305:285-298.

42. Vande Vondele,S., J.Vöros, and J.A.Hubbell. 2003. RGD-Grafted Poly-L-lysine-graft-(polyethylene glycol) Copolymers Block Non-specific Protein Adsorption While Promoting Cell Adhesion. *Biotechnology and Bioengineering* 82, No. 7:784-790.

43. Zhu,C., G.Bao, and N.Wang. 2000. Cell Mechanics: Mechanical Response, Celll Adhesion and Molecular Deformation. *Annu. Rev. Biomed. Eng.* 02:189-226.